NOVA SCHOOL OF SCIENCE & TECHNOLOGY

DEPARTMENT OF PHYSICS

Alginate hydrogels as a substrate for nerve growth

BSc in Micro and Nanotechnology engineering

Guilherme Lopes Bartolomeu

MASTER IN Biomaterials and Nanomedicine
NOVA University Lisbon
September 2023

NOVA SCHOOL OF SCIENCE & TECHNOLOGY

DEPARTMENT OF PHYSICS

Alginate hydrogels as a substrate for nerve growth

Guilherme Lopes Bartolomeu

BSc in Micro and Nanotechnologies Engineering

Adviser: Dr. Matthew Baker
Assistant Professor, Maastricht University, Principal Investigator MERLN Institute

Co-advisers: Dr. Célia Henriques
Associated Professor, NOVA University Lisbon

Examination Committee:

Chair: Prof. Jorge Carvalho Silva
Assistant Professor, FCT-NOVA

Rapporteurs: Dr. Isabel Amaral
Associate Researcher, i3S Porto University

Adviser: Prof. Matthew Baker,
Assistant Professor, Maastricht University

MASTER IN Biomaterials and Nanomedicine

NOVA University Lisbon
September, 2023

To my family

ACKNOWLEDGMENTS

I would like to express my sincere gratitude to all the professors of the Faculdade de Ciências e Tecnologias da Universidade Nova de Lisboa that accompanied me through the Master's, and to professor Célia Henriques for the feedback on the thesis. To my supervisor Dr. Ana Agustina Aldana I am deeply thankful for all her support, guidance and patience. For all her time spent explaining me everything in the most careful and attentive way, and for being a friend. To all the people at the MERLN Institute that welcomed me at their workplace with the upmost kindness, thank you. To Dr. Matt Baker, Dr. Paul Wieringa, soon to be Dr. Adrián Seijas-Gamardo, and PhD candidate Enrique Escarda-Castro I want to acknowledge all the help and guidance provided.

To my parents, for all the emotional and monetary support over the five years spent at the university, I am forever in dept. A deep thank you to my grandparents for all the support and food they gave me. I also want to thank all my friends for all the good moments shared together, and to Maria a very special thanks for all you have done.

"Opportunities multiply as they are seized."

(Sun Tzu)

Abstract

The World Health Organization (WHO) stated that neurological diseases affect up to one billion people worldwide. Accidents also provoke serious damage that goes beyond repair. Therefore, the need to create new and innovative methods to regenerate the nervous system and create proper models to study the different diseases arises. Currently, there is a scarcity of approaches that allow us to regenerate nerves. In this context, this project aimed to create a 3D scaffold for neural tissue engineering. Alginate is a very abundant biomaterial, biocompatible and hydrogels with alginate can be simple to synthesize. In this project alginate was crosslinked with calcium, creating hydrogels with ionic crosslinking, and alginate hydrogels crosslinked with adipic acid dihydrazide and bishydroxalamine to form hydrazone and oxime bonds, respectively, were also used (DCvC). We hypothesized that the properties of the dynamic networks would facilitate axon outgrowth in a 3D environment. In this project it was possible to do an extensive material characterization of alginate hydrogels, which allowed to observe how much versatile the properties of these hydrogels can be. It was possible to obtain hydrogels with distinct young modulus (≈2kPa to 70 kPa) and stress relaxation values (277 to 1385s half-time relaxation), using the same crosslinking chemistry. These hydrogels showed potential to be used for culture for every type of soft tissue. However, it is still necessary to resolve some problems regarding stability during culture and degradation. For the cell experiments PC12's and nociceptor spheroids were used. With the PC12's, it was possible to achieve some axonal growth, and also see how the dynamic hydrogels allowed for the cells to penetrate and move inside of the hydrogels. While for the spheroids culture the importance of hydrogel stability proved crucial for cells to attach and grow, and it was not possible to observe axon growth in replicated experiments.

Keywords: Alginate hydrogels, Nerve Cells, Axons, Dynamic network

RESUMO

A OMS afirmou que doenças neurológicas afetam à volta de um bilião de pessoas mundialmente. Não apenas doenças, mas também acidentes por vezes causam danos irreversíveis no sistema nervoso. Devido a isto aparece a necessidade de criar métodos inovadores para a regeneração do sistema nervoso, e novos modelos para estudar estas doenças. De momento existem poucas estratégias para regenerar nervos. Dito isto, este projeto foca-se em criar um *scaffold* 3D para servir como substrato para atingir crescimento de nervos. Alginato é um biomaterial abundante, biocompatível e hidrogéis de alginato podem ser sintetizados por uma abordagem simples. Neste projeto as cadeias de alginato foram reticuladas utilizando cálcio, criando assim uma reticulação iónica, foram também utilizados di-hidrazida do ácido adipico e bishidroxalamina, que formam ligações hidrazida e oxima, respetivamente (DCvC). A hipótese do projeto é fundamentada na possibilidade de que as propriedades das ligações dinâmicas que formam o hidrogel facilitem o crescimento de axónios num ambiente em 3D. Durante o projeto foi possível realizar uma extensa caracterização dos hidrogéis de alginato, o que permitiu observar a versatilidade das propriedades destes geís. Foi possível obter hidrogéis com módulos de Young distintos (≈2kPa-70kPa) e também diferentes valores de relaxação de stress (277 até 1385s tempo de meia relaxação), utilizando a mesma química para realizar a reticulação. Estes hidrogéis mostram assim potencial para serem utilizados para a cultura de qualquer tipo de tecido mole. No entanto, ainda é necessário resolver alguns problemas relativos à estabilidade durante a cultura e a degradação do hidrogel. As experiências com células foram realizadas com PC12's e esferoides de nociceptores. Com as PC12 foi possível observar crescimento de axónios, e também observar como o hidrogel dinâmico permitia às células penetrar e mover-se dentro dos hidrogéis. Para a cultura com os esferoides demonstrou ser muito importante a estabilidade do hidrogel para permitir a adesão e crescimento das células, e não foi possível observar o crescimento de axónios em experiências replicadas.

Palavras-chave: Hidrogéis de alginato, Nervos, Axónios, Reticulação dinâmica

CONTENTS

LIST OF FIGURES

List of Tables

GLOSSARY

Amoeboid Movement	A crawling-like type of movement that cells can do
Dynamic Crosslinking	Crosslinking created by reversible reaction, therefore able to attach and re-attach after rupture

.

ACRONYMS

CNS	Central Nervous System
DCvC	Dynamic-Covalent Chemistry
ECM	Extra Cellular Matrix
GPC	Gel Permeation Chromatography
HMW	High Molecular Weight
LMW	Low Molecular Weight
NGF	Nerve Growth Factor
NMR	Nucleic Magnetic Resonance
PNS	Peripheral Nervous System
RGD	Arginylglycylaspartic acid

SYMBOLS

L_O.Alg_5wt%_1.0:0.0 This is the way hydrogels are referred to in graphs, the initial L represents the Low Molecular Weight Alginate, then O.Alg refers to the oxidized alginate. The 5wt% is the polymeric content and the 1.0:0.0 is the crosslinking ratio of hydrazone and oxime bonds.

H_O.Alg_2wt%_0.6:0.4 The initial H represents the High Molecular Weight Alginate, then O.Alg refers to the oxidized alginate. The 2wt% is the polymeric content and the 0.6:0.4 is the crosslinking ratio of hidrazide and oxime bonds.

H_Alg_3wt%_Ca20mM The initial H represents the High Molecular Weight Alginate and can be changed by an L to represent the Low Molecular Weight. The Alg means it is a hydrogel of alginate, Ca because it is crosslinked with Calcium and 20mM represents the concentration of crosslinker

1

INTRODUCTION

The nervous system is widely studied all around the world and triggers a lot of interest since it is comprised of differentiated cells with little to no capacity of regeneration in evolutionary higher organisms, such as humans. [1] Several diseases, can affect both the Central Nervous System (CNS) and the Peripheral Nervous System (PNS). Currently, there are not many approaches to cure them, [2] with all existing treatments focusing mainly on making them more tolerable on a day-to-day basis. [3] Because of these problems, new approaches are being researched [4,5] to make it possible to comprehend how to regenerate the nervous system and create models of diseases, so we can understand them to a further extent. With this project, we sought out to achieve neuron growth in a 3D environment, utilizing a well-known biomaterial (alginate) in the form of hydrogels. Hydrogels have been widely studied [6-11] due to their capabilities of recreating the physical properties of the extracellular matrix and helping understand how cells behave.

1.1 Nervous System

The human nervous system (Figure 1.1) is traditionally divided into the central nervous system (CNS) and the peripheral nervous system (PNS). They are comprised of a network of neurons. The CNS is composed of the brain the spinal cord and optic nerve, its roles in the human body are to process and integrate information, decision-making, and initiation of actions; signaling within the nervous system enables feeling, language, memory, thinking, and all other functions and sensations. [12] The PNS is composed of efferent neurons, which transmit the signals from the CNS to the body, and afferent neurons, that transmit signals from the body to the CNS. In mammals, neurons from the central nervous system are incapable of regenerating, and [13]

this can primarily be attributed to postinjury glial scar formation at the site of injury. This creates an inhibitory microenvironment of extra cellular matrix (ECM) components, preventing the successful regeneration of the CNS. [14]

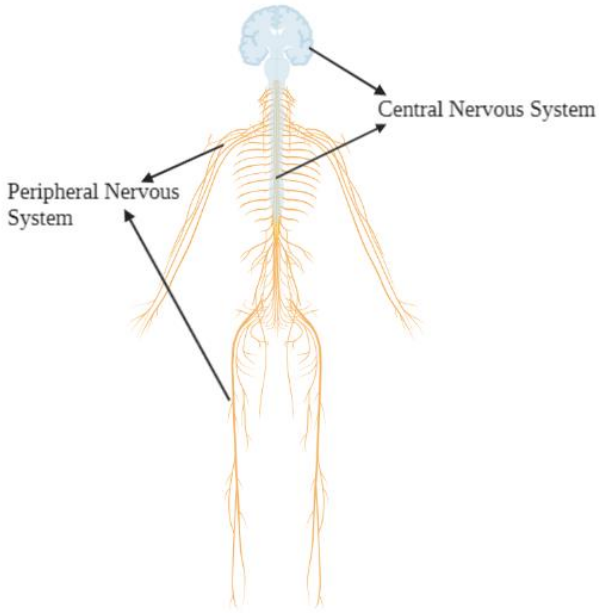

Figure 1.1 - The Nervous System, highlighted are the Central Nervous System and the Peripheral Nervous System

On the other hand, the PNS exhibits regenerative capabilities and is more responsive to therapeutic intervention. After peripheral nerve injury, axons can regenerate, while the distal portion of the axon undergoes Wallerian degeneration, resulting in the fragmentation and disintegration of the axon. Meanwhile, proximal axons can regenerate and re-innervate the damaged area, allowing recovery of function.

1.1.1 Neurons

Neurons, or nerve cells, are differentiated cells that create, transmit and receive electrical signals in the body. They are composed of dendrites, cell body (soma), and an axon. (Figure 1.2) Signals are received through the dendrites, go to the cell body, and then continue along the axon until they reach the synapse - the communication point between two neurons. [15] Neurons have different roles, and they are comprised in three distinct groups, sensory: motor and interneurons. Sensory neurons acquire information about what is happening inside and outside of the body and bring the information to the CNS, while motor neurons get information from other neurons and carry commands to the muscles, organs, and glands. As for interneurons,

they receive and transmit information to other neurons. Even though they can only be found in the CNS, interneurons are the most abundant cells. [16]

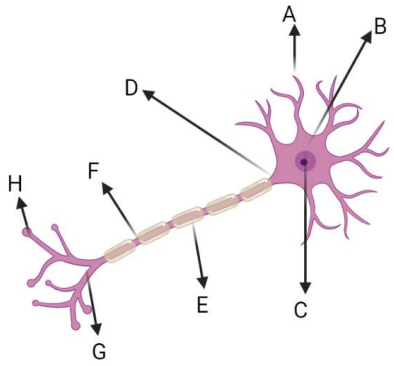

Figure 1.2 - Schematic of a neuron. A-Dendrite; B-Cell body; C-Nucleous; D-Axon; E- Myelin sheath; F-Node of Ranvier; G-Axon terminal; H-Synapse. 17 Image created in Biorender

1.1.2 Axons growth mechanisms

Neuron cells have a limited regenerative capacity, as was mentioned above. However, it is important to understand the mechanisms behind axons elongation and growth. The network that comprises the nervous system relies greatly on axons propagating the information in the form of action potentials. Depending on the structure of the glial cells that envelop the axons, they can be divided into two groups: unmyelinated axons and myelinated axons. Axons are very long and thin, reaching lengths up to 2 meters in humans, with a diameter rounding 1 μm. They grow when the hippocampal and cortical excitatory neurons polarize: when this happens a single neurite starts growing rapidly, while the other neurites see their growth be restrained. These neurites will later form dendrites.[18] It was shown, later that doing actin depolymerization using cytochalasin or latrunculin, the restrain in polarity disappears, and instead of one axon, several axons can initiate their growth. [19] This growth mechanism uses a growth cone; this is an actin-based structure found at the end of a growing axon. These growth cones facilitate axon growth and give guidance by bundling and extending actin filaments, filopodia and micro spikes. The filopodia and adhesion receptors bind to components of the ECM or ligands. Axons grow towards the target to where the filopodia attached, in a process described as the axon pulling the substrate to extend. [20] Only recently it was discovered that 3D growth cones can extend axons independent of pulling forces on the substrate and without the need for adhesion. This means that axons can grow using amoeboid mechanisms. [21]

1.1.3 Neurons extracellular matrix (ECM)

Neural stem cells, neurons, and glia all express receptors that interact or mediate interactions with specific extracellular matrix molecules. The ECM is composed of glycosaminoglycans, proteoglycans, and fibrous proteins. Some well-known components are Laminins, Collagens, and many others. [22] Collagen, for example, has been widely used in various strategies to repair nerve damage. [23] Other works have demonstrated that manipulating components of the ECM can play a key role in healing and regeneration of neurons. [24,25]

1.1.4 Mechanical properties on brain tissue

The native brain is a very soft, nonlinear, viscoelastic, solid material. It has a Young's modulus value ranging from 0.5-10kPa. [26-28] Therefore, it is expected that neurons can grow better when seeded in a soft environment. Moreover, some articles have shown that materials with faster times of stress-relaxation also seem to improve neurogenesis. [5,29] The hydrogels used during this project were expected to be soft and have viscoelastic behavior because of the dynamic networks used for the hydrogel crosslinking. Morgan, *et al.* had already reported oxidized alginate hydrogels crosslinked with adipic dihydrazide that had a stress relaxation profile in the same order of magnitude as the native tissue of the brain. [30]

1.2 Current Strategies for Nerve Regeneration

Different approaches have been employed to try to tackle the problems of nerve regeneration in the PNS, both in vitro and in vivo. Nonetheless, it is still hard to overcome the current gold standard in use, the autografts, and allografts. [31] Autografts are used to bind nerve injury gaps, and their success is attributed to the presence of Schwann cells, that offer exceptional support for orientated axon regeneration, and to the presence of great structural cues. [14] The process requires surgery, by removing an autograft from another nerve of the patient's body. It utilizes a functional but less influential nerve, this contributes to a stimulating and permissive environment, and adhesion molecules that promote neurogenesis. [32] It still presents limitations regarding various issues, such as doner site morbidity, the need for additional surgical procedure, scarring, possibility of painful neuroma, and the narrow viability of the graft tissue. [33] Allografts are an alternative for autographs when the nervous damage is superior to the critical size (3 cm in humans). Nevertheless, this technique requires 18-24 months of

immunosuppressive therapy post implantation, which can cause other problems such as infections. [14] Hollow nerve guide conduits (NGC) are a clinically approved alternative to the autografts, obviating the need of a second surgery. It can achieve the same results for small "subcritical" gaps (3-10 mm), being limited to a critical nerve gap around 3 cm in primates. [34] Sizes above this have demonstrated deficient levels of regeneration. [35] An ideal nerve repair device should be able to direct axon growth from the proximal to the distal end of the nerve, have a small pore size (5-30um) to control the infiltration of scar tissue but still allow diffusion of nutrients and the exit of waste products, have appropriate mechanical properties for the regeneration process, and possess stability. Moreover, it should have an optimal microenvironment, promote cell-surface interactions; be composed of biocompatible materials, and have suitable biodegradability for the device to be completely absorbed by the body. Lastly, the device should sustain an acceptable shelf life, be resistant to sterilization techniques, and not trigger the body's immune response. [14]

1.2.1 Materials and fabrication methods scaffolds

As mentioned above, several strategies have been studied to achieve the characteristics necessary for nerve repair. Many biomaterials (both synthetic and natural) are being used in research and are showing promising results. Some synthetic biomaterials are, for example, PLA, PLLA, PGA, PCL. [36,37,38] Natural biomaterials have also shown promising results of nerve regeneration, such as chitosan and alginate. [39,40] Endogenous biomaterials to the ECM, as are Collagen, Fibrin, Laminin, and Hyaluronic acid, [5,41,42] are widely studied as well for nerve tissue engineering. All these materials can also be used to produce the most varied substrates for nerve tissue engineering. Some studies [41,43,44,45] show substrates made of fibers (filaments and nanofibers) and structurally patterned interlumens, which can be produced using different materials and different techniques. In this project, the focus is on a different approach - hydrogels. [46,47] They can be synthesized using simple fabrication techniques and several different biomaterials, but they do not present the best level of biomimicry compared to other approaches. [14] Hydrogels can be tuned in to have physical properties similar to several native tissues, allowing the creation of 3D environments that can mimic the ECM. Moreover, hydrogels can retain considerable amounts of water - swelling -, mimicking the hydrated ECM microenvironment. The mechanical properties of hydrogels can also greatly affect cell viability and behavior. [48] To achieve neurite outgrowth in hydrogels, it is helpful that the hydrogel network can be remodeled to allow the axons to grow across the hydrogels. Moreover, it is also necessary to have adhesion points for the cells in the hydrogel since they usually do not grow in

suspension. [49] When using hydrogels made of ECM proteins, they usually already have natural cell adhesion. However, exogenous, or synthetic biomaterials must be modified to incorporate cell adhesion. [14] To facilitate matrix remodeling, dynamic network can be implemented to synthetize the hydrogel. This will create a network full of cleaving sites that can reattach the crosslinking after cleavage, allowing the cells and axons to move and grow more freely than in dense hydrogels crosslinked with a fully stable network.

1.3 Alginate

Alginate has proved to be a very useful biomaterial, which has already found numerous biomedical applications. Research has been done regarding delivery of small drugs and protein delivery, wound dressing, and cell culture, among others. [50,51,52] It is an anionic polymer that is usually extracted from the cell walls and intracellular spaces of brown seaweed, being the most abundant marine biopolymer and one of the most abundant in the world. It is commercially available with different molecular weights, reaching from 32000 to 400000 g/mol. [51] The different molecular weights allow us to have solutions with different physical properties, and consequently also hydrogels with different properties. Alginate is non-degradable in mammals since they do not have the enzyme alginase to cleave the polymer chains. The average weight of commercially available alginates is higher than the renal clearance threshold of the kidneys. [53,54] One approach to make alginate more degradable in physiological conditions is the oxidation of the alginate chains, which is usually done with sodium periodate. During the oxidation process (Figure 1.3), the carbon-carbon bond of the cis-diol group in the uronate residue alters the conformation to an open-chain adduct, enabling the degradation of the alginate backbone. The oxidation of an uronate unit generates two aldehyde moieties.

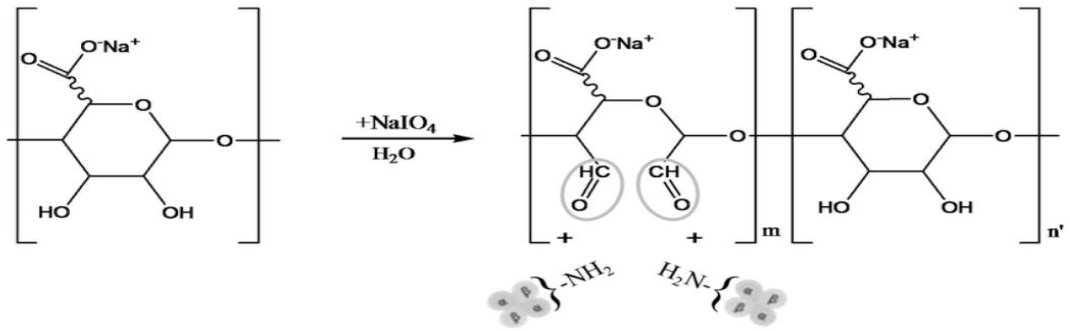

Figure 1.3 - Alginate oxidation with Sodium Periodate [55]

During this process, it is expected a decrease in molecular weight of the polymer chains since the chains are cleaved during the oxidation. The degradation rate is then very dependent on the oxidation rate, due to a higher degree of cleavage in the polymer. Factors as pH, temperature, and whether the reaction is done in an opened or closed container will influence the oxidation procedure.

1.3.1 Alginate hydrogels

In biomedicine, alginate is usually used in hydrogel form. Alginate hydrogels can be produced using different types of crosslinkers, and by doing this it is possible to achieve different hydrogels with varied properties. The most common method to prepare hydrogels with an alginate solution is to do an ionic cross-linking of the polymeric chains, with Ca^{2+} ions, for example. (Figure 1.4) This divalent cation is believed to bind to the guluronate blocks of the alginate chains, given that the structure of these blocks allows a high degree of coordination of the divalent ions. The guluronate blocks form junctions with adjacent guluronate blocks, being called egg-box model of crosslinking. [51]

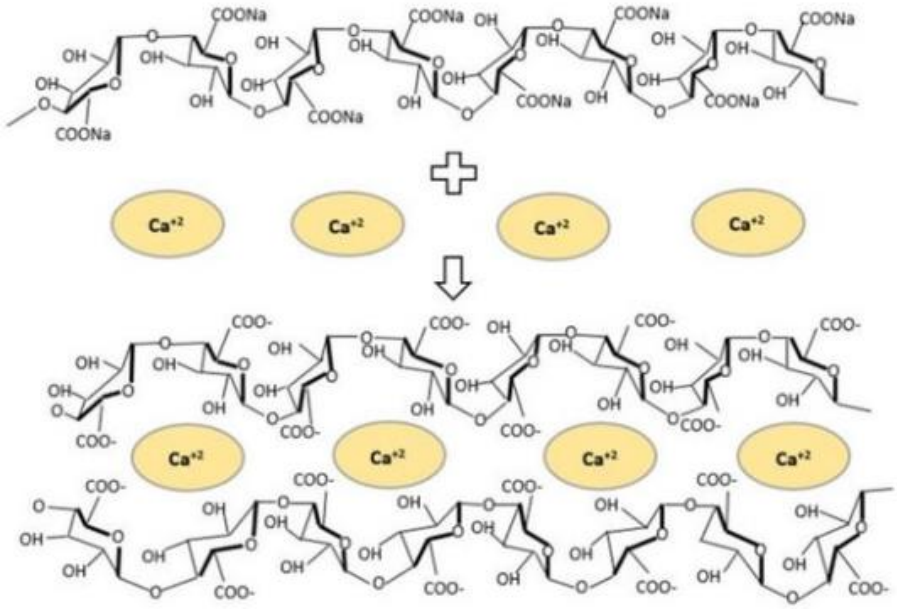

Figure 1.4 - Alginate crosslinked with Calcium, egg-box model [56]

When looking to improve the physical properties of alginate hydrogels, covalent cross-linking is an interesting option. In this cross-linking approach, it is possible to have both static-covalent, and dynamic-covalent cross-linking. Static covalent bonds usually are kinetically stable and stronger and, after rupturing it is not possible to recover the bond. However, dynamic covalent bonds can usually be cleaved more easily, but have the capability to bind again after

cleavage, similar to what happens in ionic bonds. Due to the dynamic covalent bonds being formed by reversible interactions between molecules, the bonds are said to be more dynamic when the reverse rate constant of the reaction is higher (k_{-1}). Different crosslinking molecules, even when very similar, will cause changes in the hydrogels' properties, due to changes in rate constants and equilibrium. [57] There are a lot of different crosslinkers available to cross-link alginate, and in this project the alginate was oxidized so that cross-linking could happen between adipic acid dihydrazide (ADH) to create hydrazone bonds and bishydroxalamine to create oxime bonds (most and least dynamic, respectively). The amine groups on the end of each molecule binds to the aldehyde on the alginate backbone created by the oxidation process. (Figure 1.5)

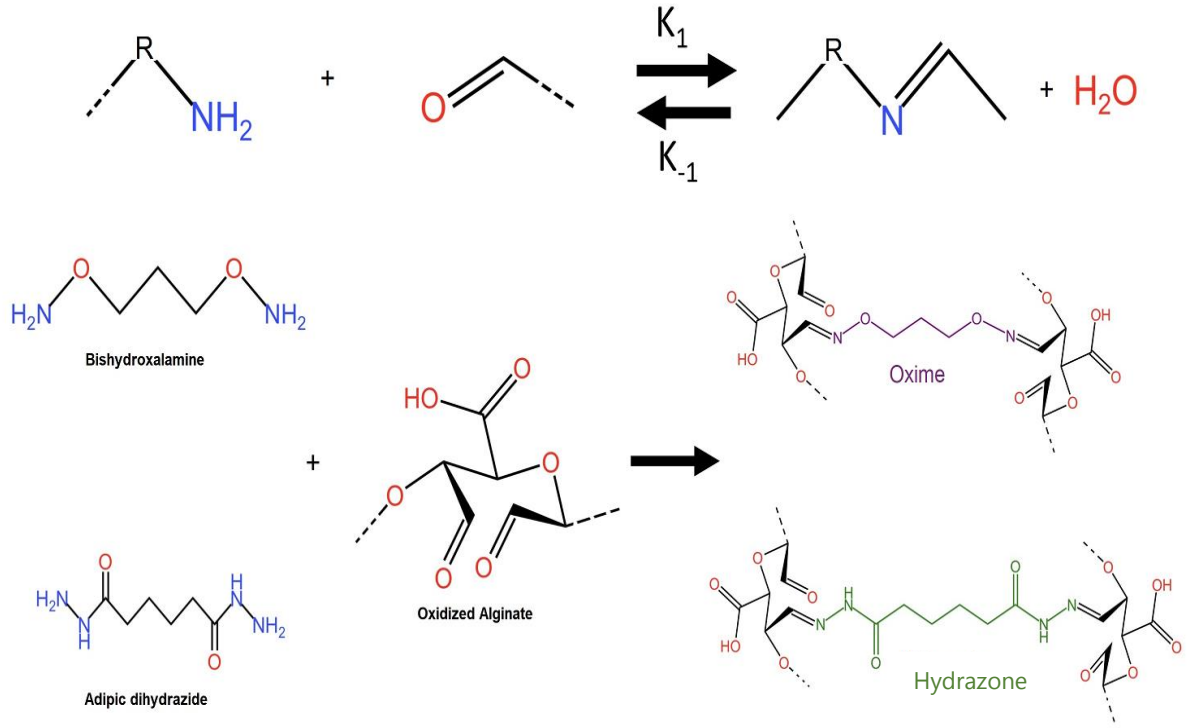

Figure 1.5 - Formation of secondary aldimines from functional groups terminated in an aldehyde and amine. Variations of the R will lead to different rate constants and equilibrium of the reaction. In this Image are represented the crosslinking reactions between the oxidized alginate chains and adipic acid dihydrazide and bishydroxalamine

The equilibrium constant (K_{eq}) is proportional to the stiffness and number of cross-links of the hydrogel. It is the quotient between the forward rate constant (k_1) and the reverse rate constant (k_{-1}). The forward rate constant is related to self-healing kinetics and rates of gel formation, and the reverse rate constant is associated with the stress relaxation behavior. [30] (Figure 1.6) Moreover, it is important to comprehend that mechanical properties of the hydrogel can be

tuned in various manners by changing the polymeric content, type of crosslinker, concentration of crosslinker, and the molecular weight of the polymer. In this project, RGD was added to the polymeric backbone to introduce adhesive sites for cells.

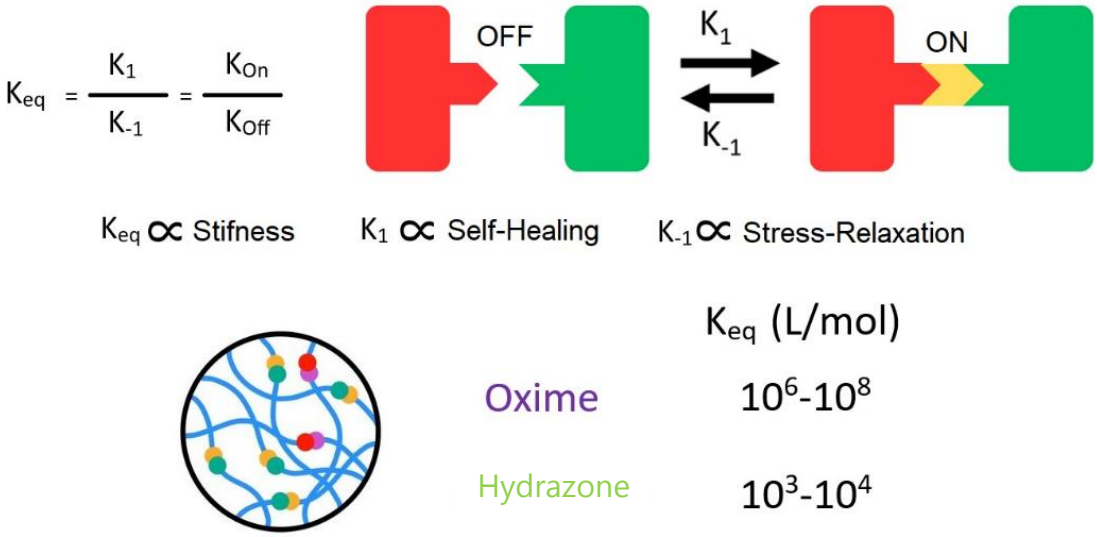

Figure 1.6 - Dynamic bonds leverages the relation between equilibrium constants, and therefore influence mechanical properties.

1.4 Cells

To study the influence of alginate hydrogels in neurite growth, two types of cells were chosen for the project. Firstly, iPCS differentiated into nociceptors, which are cells present in bones, muscle, skin, and specialized sensory organs, and respond to potentially harmful stimuli. [58] Then moving forward with the project, it was decided to change the cell type PC12's given their facility to grow and survive.

1.4.1 iPSCs nerve spheroids

Induced pluripotent stem cells (iPSCs) are a type of pluripotent stem cell derived from adult somatic cells, and they go through a genetical reprogramming to return to an embryonic stem cell-like state. The use of these cells allows us to have pluripotent stem cells without the ethical problems of using embryos. These cells then must go through a differentiation process, where they are cultured in media with the necessary promoters and inhibitors of growth factors. By the end of the protocol, the objective is to have achieved fully differentiated cells. In this project, I used neuron spheroids differentiated from human iPSCs, obtained from the Leiden Medical Center. The differentiation procedure was performed by other colleagues at the laboratory.

1.4.2 PC12s'

The PC12 cell line is frequently used for research in neuroscience, having been mentioned in various scientific papers. [59,60] There are two types of them available: the traditional PC12s' that grow in suspension, and adherent phenotype that can attach. [61] These cells grow in suspension and do not easily attach to non-coated surfaces. PC12s' are derived from rat pheochromocytoma in the rat's adrenal medulla, and they are broadly used as models in neurobiology since they exhibit features of mature neurons. [62] They are very popular in research due to their adaptability to pharmacological manipulation, simple and easy to culture and the extended knowledge that is already known regarding their proliferation and differentiation. When PC12's are cultured in the presence of nerve growth factor (NGF), they will differentiate neuron-like cells morphologically and functionally. [63] They can be used to assess neurotoxic activity of substances, which can then be assessed by cell survival, neurite outgrowth, DNA damage or protein expression. These cells can also form functional synapses between them and other neuronal cells, enabling the PC12 cells to be used in mixed cultures for research of synapse formation. [64] They were useful for this project to tackle down some issues that were appearing during the cell culture, given that they are widely used and accepted as a model for neurological diseases. The intention with these cells, as for the nerve spheroids, was to seed them in the alginate hydrogels and analyze the neurite outgrowth by assessing the axons size.

1.5 Objective

The objective of this project was to evaluate the effect of alginate-based hydrogels with different mechanical properties (elasticity and viscoelasticity) on nerve cell growth. By synthesizing polymeric networks with different molecular weight alginates, cross-linkers, and polymer concentrations, we aimed to achieve soft hydrogels with varied mechanical properties. It was hypothesized that a dynamic network could facilitate axon outgrowth because of the way those bonds facilitate network remodeling, allowing cells to move and possibly grow axons more efficiently than in hydrogels with stable networks.

2
MATERIALS AND METHODS

Two different molecular weight sodium alginates were used: FMC Manugel GMB (high molecular weight ≈ 250000), and Sigma-Aldrich, (low molecular weight ≈ 125000). Adipic Acid dihydrazide (Sigma, ≥98%), *O,O'*-1,3-propanediylbishydroxylamine dihydrochloride (Sigma, 98%), calcium chloride (Honeywell| Fluka Anhydrous, granular, ≤7.0mm, ≥93), sodium (meta)periodate (Sigma, ≥98%, $NaIO_4$), ethylene glycol (Sigma, ≥99.5%), Dulbecco's Phosphate Buffered Saline (Sigma, without $MgCl_2$ or $CaCl_2$), and dialysis membranes (VWR, Spectra/por 6, diameter = 28.6 mm, MWCO = 3.5 kDa), activated charcoal (Sigma, Norit) Filter papers (Whatman) with pore sizes 1.2 µm, 0.45 µm, and 0.2 µm, purchased from sigma. Cyclohexane (Sigma), Sodium chloride (Sigma, ACS reagent, ≥99.0%), Sodium Nitrate 0.1M to dissolve samples for GPC.
For cell culture, three different culture media were used: Neurobasal media (Gibco) supplemented with GlutaMax, High glucose DMEM (Gibco), and RPMI-1640 (Gibco). The media would then be supplemented with Fetal Bovine Serum (FBS, Sigma), antibiotics (Penicillin/Streptomycin), and Horse Serum, the supplements and the media used depends on the cells that are being used and on the experiment that is being performed. Trypsin-EDTA (0.05%, Gibco, phenol red), used as received, and formaldehyde (Sigma, 37wt.% in H_2O, containing 10-15% methanol as a stabilizer) was diluted to 4wt% in PBS before usage as fixation agent. To perform the cellular staining the following were used, calcein AM (Invitrogen) for Live/Dead, Deep Red Cell Tracker (Invitrogen), Hoechst 33 342 trihydrochloride for Live/Dead, and Propidium Iodine (PI) for Live/Dead assay, Alexa Fluor 488 Phalloidin (Invitrogen) (Dissolved in PBS In a ratio 1:200) and 4',6-diamidino-2-phenylindole dihydrochloride (DAPI, Sigma, ≥95.0% (HPLC) (Dissolved in PBS 1:250). Oxime-RGD binding peptide((AOAC)-GGGRGDS Chinapeptides, 98.05%, molecular weight = 677.65 g mol^{-1}) was used to improve cellular adhesion. Acetic Acid (Lot:1504608868, 99-100% glacial), Rat-Collagen (Concentration)

2.1 Purification of Alginate

Sodium alginate was dissolved overnight at 4ºC in distilled water with a mixing stirrer, with a concentration of 1% (w/w). In the next day, activated charcoal was added (0.5%(w/w)) and left to stir at 4ºC for 24h. The alginate and charcoal solution were centrifuged at 7100 rcf at 5ºC for 5 minutes. Afterwards, the solution was filtered through filter paper with pore sizes: 1.2 µm, 0.45 µm, and, lastly, 0.2 µm. This process was slower for the alginate with the high molecular weight since the solution was more viscous. The filtration was done during a period of 2-3 days, and solutions were stored at 4ºC overnight. The purified alginate was then frozen and lyophilized, yielding a white fibrous powder. The yield of this purification was around 50-70%, because during filtration a lot of filters are used, leading to volume loss.

2.2 Oxidation of Alginate

Purified alginate was dissolved in a beaker with distilled water (1 equivalent) until the solution was homogenous and slightly viscous. Then, a solution of $NaIO_4$ was dissolved in dH_2O with a molar equivalent of 0.11, and on another oxidation a solution of $NaIO_4$ was prepared with a molar equivalent of 0.4. The reaction must be protected from light so before adding the $NaIO_4$ the beaker with the alginate solution was covered in aluminum and then the oxidizing agent was added all at once. The solution was left steering for 17h covered, then ethylene glycol with the 1 molar equivalent to the $NaIO_4$ was added and left to stir for 1 hour to quench the oxidation. The solution was then dialyzed in 5L of NaCl with decreasing concentration. The dialysis solution is changed usually twice a day for a total of 5 times (100; 50; 25; 12.5; 0mM). After the dialysis, the solution was frozen and lyophilized to yield a white fibrous solid. The yield of this solution was around 70%. The theoretical degree of both the oxidations were 11% for the oxidation done with a 0.11 eq of $NaIO_4$, and 40% of oxidation for the oxidation done with a 0.4 eq of $NaIO_4$.

2.3 Stock Solutions

Stock solutions of crosslinkers were prepared: For calcium chloride was prepared a stock solution with a concentration of 100mM, mixed in PBS, the adipic acid dihydrazide and the bishydroxalamine solutions were prepared with a concentration of 0.1 M, also mixed in PBS.

However, the bishydroxalamine changes the pH of the PBS (7pH), so, after dissolving, the pH must be corrected using a NaOH solution. To evaluate the pH levels, pH color strips were used.

2.4 Hydrogel Preparation

There were two distinct hydrogels used during this project. Sodium alginate crosslinked with calcium chloride ($CaCl_2$), and for these two different crosslinking concentrations were experimented (20mM and 40mM). The other hydrogel was composed of the oxidized alginate crosslinked with either only hydrazone bonds (adipic acid dihydrazide) or both hydrazone and oxime bonds (bishydroxalamine). The crosslinking concentration depends on the percentage of oxidation of the polymer. Crosslinking would always be done with the same amount of moles of crosslinker after calculating the moles of aldehydes after the oxidation (calculating the moles assuming a 10% oxidation and another one with 40% oxidation).

The preparation of the hydrogels would vary between the experience that would be performed. For swelling and porosity experiments, the hydrogels were prepared in molds with 6 mm diameter and 2.37 mm height, around 80-100 µl of solution per gel. A cover slit is placed on the bottom of the mold, then the alginate solution would be mixed with the crosslinker solution and then pipetted onto the mold. After, the top part is also covered by a cover slit and the hydrogels are left overnight to ensure the full crosslinking of the network.

For the compression and stress-relaxation experiments, the hydrogels would be prepared utilizing a bottomless 96-wellplate and 250µl of solution per gel, because for these experiments bigger hydrogels were necessary. The well plate was covered on the bottom, attached with some tape. To avoid water evaporation during the night, the well plate needs to be covered on the top after the solutions are Inserted into the wells. However, the alginate hydrogels crosslinked with calcium would crosslink relatively fast, therefore pipetting the solution was not an option. The hydrogels crosslinked with calcium were broken so that they would properly fit into the molds (for the swelling and porosity), and then left overnight to ensure that after being broken they could establish the crosslinking again. For the compression and stress-relaxation experiments, the mold that was being used was bigger, and this allowed to pipette the alginate solution before crosslinking into the wells. Then, the crosslinker would be added and mixed, already in the well. At the end of section D in supplementary information all the hydrogels' formulations experimented are presented on a table.

2.5 Swelling

The swelling experiments were performed using various hydrogel formulations with the dimensions mentioned in 2.4. The hydrogels were removed from the molds and then placed in a 24-wellplate, where they were submerged in neurobasal media. The hydrogels weight would be measured at different time points: 0, 5, 15, 30, 60, 120, 240, 480, and 1440 minutes. The swelling ratio is then calculated using the following equation:

$$S = \frac{Mt}{Mi'}$$

The mass at a specific time point - Mt, and initial mass - Mi. Swelling was done with at least three replicas for each sample. Additionally, to analyze if the dry hydrogels were able to regain their initial weight, they were put in a 24-wellplate, submerged in PBS, and their weight was measured at different time points for a period of 72h.

2.6 Porosity

To assess the porosity of the hydrogels, they were first lyophilized in the freeze drier. Using an inert liquid (cyclohexane) it is possible to calculate the empty space inside of the dry hydrogel, since the cyclohexane does not interact with the alginate. The porosity experiment was repeated three times for two replicas of each sample. Using the following equations, it is possible to calculate the porosity of the hydrogels:

$$V_{hydrogel} = 1 - \frac{(W2 - W1 - Wdry)}{\text{Density } (C^6H^{12})}$$

$$\rho_{hydrogel} = \frac{\left(\frac{Wdry}{Vhydrogel}\right)}{1000}$$

$$V_{pores} = \frac{(W2 - W3 - Wdry)}{\text{Density } (C^6H^{12})}$$

$$\text{Porosity} = \frac{Vpores}{Vpores + Vhydrogel}$$

W1- weight of the vial, W2 – weight of vial, dry hydrogel, and 1mL of cyclohexane, W3 – weight of vial and the cyclohexane, and Wdry - the weight of the dried hydrogel.

For this experiment to be more accurate it is better to utilize scaffold samples with a weight of the same order of magnitude of the vial.

2.7 SEM

To corroborate the results obtained in the porosity experiment, the hydrogels were cut in half and images of the cross-section were analyzed with SEM. The dry hydrogels were placed in proper supports and glued down using conductive carbon tape. After having the hydrogels in the proper supports, they must be coated with a gold layer so that the hydrogel becomes conductive, and it is possible to image it using SEM. The imaging was performed only once on one replica of each sample. The pore sizes were afterwards analyzed using the Fiji software (Distribution of ImageJ).

2.8 Mechanical compression testing

2.8.1 Compression

Compression data was obtained using the Mechanical tester (TA Electrofor Model: 3230-ES series III), and a Load cell with a maximum load capacity of 45N. The hydrogels dimensions were measured (diameter and height in mm), and then from the machine data regarding Load (N) and displacement (mm) were obtained. This way it is possible to calculate the strain and stress using the following equations:

$$Strain(\%) = \frac{Displacement(\mathrm{mm}) - InitialDisplacement(\mathrm{mm})}{Height(\mathrm{mm})} * 100$$

$$Stress = \frac{Load(\mathrm{N})}{SurfaceArea(\mathrm{mm^2})}$$

For the experiment to be optimal, the hydrogels should all be the same size, therefore they were all prepared using the same mold and the same volume. The hydrogels were compressed at a rate of 1% per second, where 100% corresponds to the total height of the hydrogel. They were compressed up to 70% of their total height to ensure full failure of the hydrogel. Each sample evaluated during compression before and after swelling had five replicas. However, some of them did not provide trustworthy results and were excluded from the final calculations of mean that are presented in the graphs in the results section.

2.8.2 Stress-Relaxation

The stress-relaxation measurements were also done using the mechanical tester, but this time using the most sensitive load cell with a max load capacity of 1000g or approximately 10N. To perform this experiment, the hydrogels were all measured as for the compression experiments, but the graphs obtained are stress over time. The hydrogels were compressed up to 30% of their total height. This value was chosen because lower values of compression had a very noisy signal. The compression was done carefully at a rate of 1% per second and the load values were measured over a period of 3 hours. Nonetheless, when the load values became negative the experiment would be stopped, since there was already no load being applied to the cell. Because the load cell used gave data of load in grams, to use the equations mentioned above, the Load (N) had to be calculated using F=m*g. For this experiment, three replicas per sample were done.

2.9 Cells

2.9.1 Alginate +RGD

RGD was added to the polymer backbone to help with cell adhesion. For the alginate hydrogels RGD was added following the following protocol: alginate (250mg) was added to a flask and MES buffer (0.1M, pH6), biotin (39g) is dissolved In 6mL solution of MES buffer; DMTMM (349.55 mg) is added to the first flask, then 25.2 µL of a 100mM RGD solution is added and left to stir overnight. After this the solution must be dialyzed using the same filters mentioned in the alginate purification section. For the oxidized alginate this process is simpler since it is only necessary to add the oxime-RGD solution to the alginate solution before preparing the hydrogels because the RGD will bind to the aldehyde groups in the oxidized alginate.

2.9.2 PC12s' cell culture and differentiation

To perform the PC12's culture, the cells were cultured in a T75 flask with RPMI-1640 media, supplemented with 10% horse serum and 5% FBS. These cells grow in suspension so, to perform the media changes (every 2-3 days), the cells needed to be centrifuged at 200 RCF for 5 minutes previously to the media removal. To split cells that are clustered together in suspension, the culture media was pipetted up and down through a syringe with an 18G needle. To perform the priming (differentiation) of the cells before seeding them in the hydrogels, a 6-

wellplate was coated with a solution of rat collagen 250µg/mL in 0.02M acetic acid and left overnight. The day after, the solution was removed and the cells seeded (around 2x10^5 cells seeded per well), attaching to the collagen. The cells were left for 7 days in DMEM high glucose media with 100ng/mL of NGF, and the media changed every 2 days. After 48h, it was already possible to see the PC12s growing axons, but they were left in those conditions for a full week to ensure the highest number of primed cells. On the 7th day, the cells would be detached using trypsin and counted, so that they could be seeded in the hydrogels.

2.9.3 Preparation of the hydrogels for cell culture

To prepare the hydrogels for cell culture different approaches were used. To sterilize the hydrogels, they were irradiated with UV (265nm wavelength) for 10 minutes. This approach worked for most of the project, since no contaminations were observed in culture. However, later contaminations started to appear, to prevent this every solution used to prepare the hydrogels was filtered through a 0.2 µm filter, and the hydrogels prepared inside a flow hood. The hydrogels used for culture of the PC12's cells were prepared directly in a 96-wellplate adding 50 µL of the hydrogel solution (Alginate dissolved in PBS + the corresponding cross-linker, depending on the hydrogel formulation) to the bottom of the wells. For the spheroid culture the hydrogels were prepared also in a 96-wellplate, but using more volume, 100 µL per hydrogel, the strategies used for the culture of the spheroids are demonstrated on figure 3.13. The strategy that was used in most of the experiments was the one demonstrated on figure 3.13 C, which was named as sandwich strategy. With this strategy the hydrogels were placed on the bottom of the well, the spheroids were removed from solution and inserted on top of that hydrogel and another hydrogel placed on top, to always ensure contact between the spheroids and the hydrogels using the scaffold to culture the cells in a 3D environment. To improve cell adhesion to the alginate hydrogels RGD was added to the backbone of the polymeric chains before preparing the hydrogels (0.05 µL or 1 µL of RGD solution per 100 µL of hydrogel, the value was increased in later experiments).

2.9.4 PC12s´ culture in hydrogels

A suspension of cells was pipetted directly onto the top surface of the hydrogels that were crosslinked inside a well of a 96-wellplate (50µL of hydrogel solution). Since these cells are significantly smaller size than the spheroids, the cells would just travel inside of the scaffold. 4000-5000 cells were seeded per hydrogel because increasing the number of cells leads them

to cluster very rapidly, and, when they cluster, they do not always grow axons. This clustering was observed on other experiments performed; these results are not presented in the thesis. Another reason to choose this number was because of the recommendation number given by ThermoFisher when using 96-wellplates and previous work performed in the laboratory. The media used for the culture in the hydrogels was High Glucose DMEM with 1% (v/v) Horse Serum, 100 µg/mL penicillin and 100 µg/mL Streptomycin and 100 ng/mL NGF. To each well 100 µL of media were added and changes were performed every 48h, removing all the media present in the well and adding more 100 µL. The staining done on the PC12's was performed before they were seeded in the hydrogels, using Deep Red cell tracker resuspended in 20µL of DMSO. The staining solution was added to the cells with a dilution of 1 µL per each 1mL of media, and then the cells would be kept in an incubator for 15 to 20 minutes. The Deep Red Cell Tracker passes through the membrane of the cells and reacts with the amine groups in proteins. The culture would be maintained for a 3 to 4 days period with daily tracking of the cell's growth. Cell culture was performed using at least three replicas for each hydrogel sample where cells were being seeded in. The control utilized for these experiments were made by seeding the PC12's in wells coated with collagen. To coat the wells the same solution used for the differentiation of the PC12's was used (rat collagen 250µg/mL in 0.02M acetic acid).

2.9.5 PC12's Live/Dead assays

Two different Live/Dead assays were performed on PC12 cells after seeding them on the hydrogels. One of the live/dead assays was performed after 24h of cell culture in the hydrogel, taking advantage of the Deep Red Cell tracker that stained all the cells present in the hydrogel, and calcein am (dissolved in PBS at a ratio of 1:1000) to stain the viable cells in a green color. The media from the cells is removed, and the staining solution is added to each well, and left to incubate for 30 minutes at 37ºC. The wells are then washed with PBS and culture media is added to cells before taking them to the microscope. The other live/dead assay was performed after 96h of culture of the PC12's in the hydrogel using Hoechst (blue) to stain all the cells, and Propidium Iodine, PI, (yellow) to stain the dead cells. This procedure is slightly different because the staining agents were mixed in high glucose DMEM instead of PBS, to try to maintain the cells in an environment more fit for them. Then the cells were incubated for 30 minutes at 37ºC. After the incubation period the staining solutions are removed, and high glucose DMEM is added to the wells, before taking the cells to perform microscopy. For both Live/Dead assays

the microscopy was done with the microscope that had environmental control to maintain the cells at 37ºC and 5%CO2.

2.9.6 iPCS Neuron spheroids culture in hydrogel

The human iPCS line LUMC0031iCTRL08 (Provided by the Leids Universitair Medisch Centrum IPSC core facility) were used already differentiated into nociceptors cells, which formed spheroids of cells. Experiments seeding these spheroids in 2D, and 3D were performed. To ensure the encapsulation of the spheroids in the hydrogel, a sandwich approach was done. Placing one hydrogel on the bottom of the 96-wellplate, then inserting the cells onto the hydrogel, and covering it with another hydrogel. At least 5 spheroids needed to be placed in each well according to previous experiences performed with these spheroids, because less than that would create difficulties in finding the spheroids while imaging. For the culture of this cells, Neurobasal media with GlutaMax was used, complemented with Penicillin (100µg/mL) and Streptomycin(100µg/mL), and NGF at a ratio 1:1000 (100ng/mL). The cells were usually seeded in the hydrogels for 1 week, initially adding 100 µL of media per well, and having media changes every 48h. Due to hydrogel swelling, the amount of media changed depended on how much media it was possible to remove, and then how much media was possible to add before filling up the wells. Later, the experiments were shortened, because of structures on the hydrogels that started appearing after 3 to 4 days that were associated to hydrogel degradation. To fixate the spheroids the media was removed, and a 4% formaldehyde solution was added and left for 30 minutes at around 21ºC (room temperature), rinsed with PBS and left in PBS. To perform the cell staining phalloidin was used to stain the cells actin filaments, and DAPI to stain the cell's nucleus. The phalloidin solution was prepared dissolving phalloidin in PBS at a ratio of 1:200. The staining was performed by submerging the hydrogels with the cells for 30 minutes in the phalloidin solution. The DAPI solution was prepared by dissolving DAPI in PBS at a 1:250 dilution ratio (0.2 µg/mL) and then submerging the hydrogels for 5 minutes. After staining the cells were left in PBS. Cell culture was performed using at least three replicas for each hydrogel sample where cells were being seeded in.

2.10 Microscopy

As mentioned for the spheroids the cells were stained and left in PBS, and then taken to the microscope. The PC12's were just removed from the incubator and taken directly to the microscope that had environmental control. The imaging of the spheroids was done in an Inverted microscope coupled with spinning disk (Nikon Eclipse Ti-e) equipped with a Lumencor Spectra light source, an Andor Zyla 5.5 sCMOS camera (monochromatic for fluorescence) a Nikon DS-Ri2 color camera, and an MCL NANO Z200-N TI z-stage. To perform the imaging of the PC12's the same microscope was used but with environmental control to maintain the cells at 37ºC and 5% CO2 environment. The images obtained from the microscopy were analyzed using Fiji software (a distribution of ImageJ). It was essential to place scale bars on the images and remove the background from the fluorescent images. The amplifications used are present in the images presented in chapter 3.6.

2.11 Statistical analysis

The number of samples used in each experiment is stated in the correspondent section in the Materials and Methods chapter. Statistical significance between two samples was assessed using Student's t-test for independent sample populations with different variations in Microsoft Excel. Significance differences were set at $p < 0.05$. The statistical analysis can be seen in A in supplementary information.

EN: "The research work described in this dissertation was carried out in accordance with the norms established in the ethics code of Universidade Nova de Lisboa. The work described and the material presented in this dissertation, with the exceptions clearly stated, constitute original work carried out by the author."
PT: "O trabalho de investigação descrito nesta dissertação foi realizado de acordo com as normas estabelecidas no código de ética da Universidade Nova de Lisboa. O trabalho descrito e o material apresentado nesta dissertação, com as exceções claramente indicadas, constituem trabalho original realizado pelo/a autor/a. "

3

Results and Discussion

This project is focused on the production of alginate hydrogels with dynamic networks, with the hypothesis that the dynamic network would facilitate neurite outgrowth, and axon elongation. Two crosslinks were used, ionic crosslinking (by mixing alginate with calcium) and covalent-dynamic crosslinking. For the covalent-dynamic, two different cross-linkers were used: adipic acid dihydrazide (to form hydrazone bonds) and O, O'-1,3-propanediylbishydroxylamine dihydrochloride (to form oxime bonds). For this work, two different alginates were used with two distinct molecular weights. They are named as the low (LMW) and high molecular weight (HMW) alginates. The oxidation of both LMW and HMW was carried out targeting 10% oxidation degree. By GPC, the values of the molecular weight of the alginates, before and after oxidation, were assessed. The GPC graph and the molecular weight values, as well as the corresponding dispersity, are shown in figure 3.1. After oxidation (11% - theoretical), the molecular weight decreased in half for both polymers. This is expected due to the cleavage of the polymeric chains during the oxidation process. This creates the aldehyde bonds in the polymer backbone, allowing the crosslinking of the polymer and the bioconjugation of bioactive molecules/peptides (oxime-RGD).

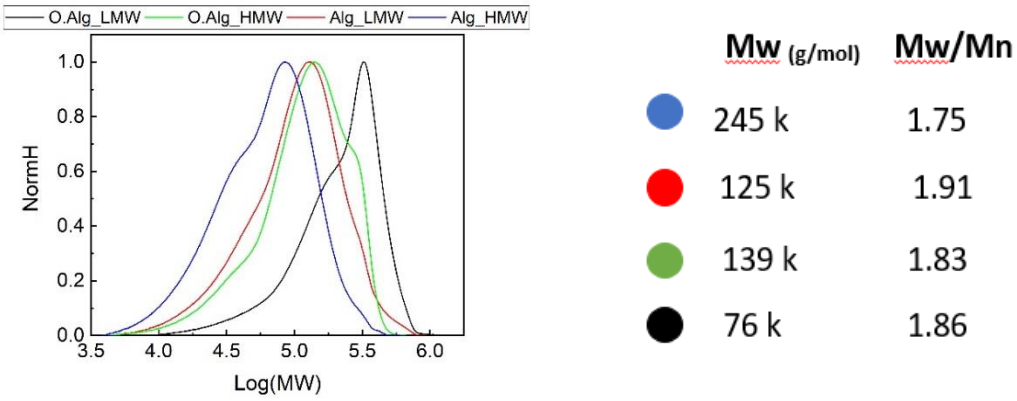

Figure 3.1 - GPC graph and the obtained Molecular Weight of the different Alginates and Oxidized Alginates

The molecular weight of both alginates differs from each other by a factor of approximately 2. When oxidized, this relation is maintained, but with a slight difference (1.81 factor). To also verify the oxidation of the alginate chains, a Nucleic Magnetic Resonance spectroscopy (NMR) was performed. The NMR analysis can be found in C in the supplementary information. The GPC and NMR analysis were not performed for the alginate oxidized to 40% because of unavailability of the machines, but it would be interesting to observe how the molecular weight of the polymeric chains' changes.

3.1 Hydrogel formulation

We first explored the polymer concentration and the crosslinking density for the hydrogel's preparation. A PBS buffer was used to keep the pH at 7. For the oxidized alginate hydrogels, the crosslinking density depends on the oxidation degree, so it is necessary to decide on the ratio between the two cross-linkers: adipic acid dihydrazide (hydrazone bonds) and bishydroxalamine (oxime bonds). With the conclusions taken from the swelling experiments (Figures 3.2, 3.3 and 3.4), it was possible to understand which formulations were more stable. The choice of the formulations of the hydrogels was based on the handling and the ability to maintain their structure. Moreover, the degree of swelling is also a factor since more swelling can disturb the image during microscopy.

3.1.1 Alginate + Calcium hydrogels

The alginate crosslinked with calcium hydrogels were tested with a polymer concentration of 1, 2, and 3 wt%, for the high molecular weight alginate, and with a concentration of Calcium Chloride of 10, 20 and 40 mM. The hydrogels synthesized with the low molecular weight alginate had to have a much higher polymer concentration to gel, given the smaller size of the alginate chains. These hydrogels were experimented with a concentration of 7.5 and 10 wt%. The crosslinking concentrations experimented were the same as for the hydrogels made with the high molecular weight alginate mentioned previously. One problem with making these hydrogels is that, considering the high polymeric content, the ionic crosslinking, and the small polymeric chains, a brittle hydrogel that is not capable of retaining its structure is formed. After the hydrogel formation, in order to maintain its structure, the hydrogel has to be post crosslinked in a CaCl2 solution (100mM) for roughly five minutes. Based on the same criteria mentioned above, the hydrogels' formulation was chosen.

3.1.2 Oxidized alginate hydrogels

The high molecular weight hydrogels had already been studied by Morgan et.al, so the same polymer concentration was used - 2wt%. [30] The crosslinking concentration remains the same, corresponding to the molar equivalent of aldehyde bonds present in the polymer backbone. The crosslinking ratios chosen were 1.0 molar equivalent of hydrazone crosslinking, and 0.6 mol equivalent of hydrazone plus 0.4 mol equivalent of oxime crosslinking. The ratios were chosen based on the results Morgan, *et al.* obtained when doing cell experiments with fibroblasts, based on the spreading of the fibroblasts on the hydrogel. Moreover, the values for stress-relaxation of the hydrogels were also a factor when choosing the formulation. [30] The stress-relaxation values also influenced the choice, since higher stress-relaxation values have been shown to improve neurogenesis. Therefore, it was decided to keep higher concentrations of hydrazone bonds than of oxime.

The alginate with the high molecular weight was also oxidized to a degree of 40%. Since the polymeric chains are now smaller, it becomes necessary to increase the polymeric content of the hydrogels. With this degree of oxidation, the oxidized alginate would only start to gelate at 3 wt%. Based on the handling and stability of the hydrogel after 24h of swelling in media, the formulation chosen had a polymeric content of 4 wt%. The crosslinker used for this hydrogel was only 1 mol equivalent (to mols of aldehydes) of hydrazone. Due to the high increase in the crosslinking density, it did not seem necessary to also add the less dynamic crosslinker. For the oxidized alginate with the Low Molecular Weight (LMW), several polymer concentrations were experimented: 4, 5, 6 and 7 % (w/w). Using the criteria mentioned previously during the swelling experiments in media, the polymeric content chosen was 5 wt%. The crosslinking ratios experimented were 1.0:0.0 (hydrazone:oxime) mol equivalent, 0.8:0.2, 0.7:0.3, and 0.6:0.4. But, when moving forward with the project, only the 1.0:0.0 and the 0.6:0.4 ratios were kept for these are the ratios that were going to be used for the HMW oxidized alginate hydrogels. The hydrogels synthesized with the oxidized alginate have smaller polymeric chains than the other hydrogels. However, they are crosslinked by dynamic-covalent bonds, which are stronger than ionic bonds. Therefore, it is not necessary to increase the polymeric content as much for the oxidized alginate as it was for the hydrogels crosslinked with calcium. Using these two different crosslinking approaches it was possible to obtain very different hydrogels, with different mechanical properties. The difference between the hydrogels could be seen just by handling them, and it was interesting to observe different mechanisms that allow a polymer to gel and create unique materials different from each other using alginate for all of them.

3.2 Swelling

Hydrogels are biomaterials capable of retaining large amounts of water, so the analysis of the swelling variation can be very insightful in understanding how the polymer network behaves. The swelling profiles obtained for each hydrogel can be seen in Figures 3.2, 3.3 and 3.4.

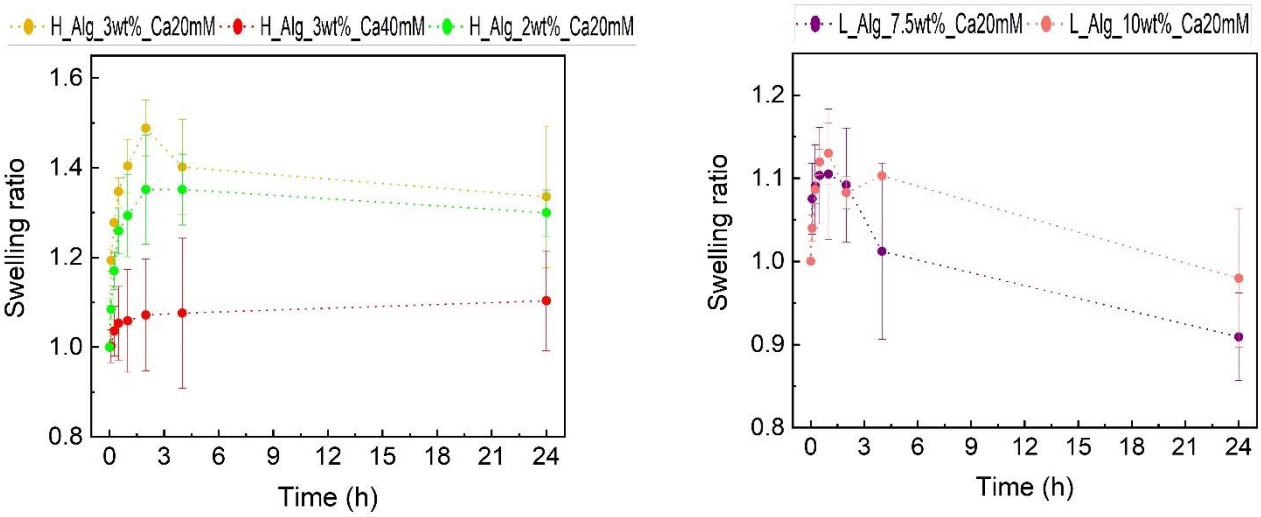

Figure 3.2 - Swelling graphs of Alginate crosslinked with Calcium, the left graph is correspondent to the hydrogels made with the High Molecular Weight, and on the left is the swelling graphs of the hydrogels made with the Low Molecular Weight Alginate

Almost all the HMW alginate crosslinked with calcium hydrogel formulations mentioned in chapter 3.1 dissolved in the media during the swelling experiment, and that is why they are not represented in the graphs. It is observable that, with a higher crosslinker concentration, the hydrogels swell less, which is expected given that the network is more compact and possesses more binding sites between the polymeric chains. Keeping the crosslinker concentration the same, the hydrogel with higher polymeric content swells more, and even though the error bars overlap between the two samples, it is still possible to see the trend. This can be attributed to the fact that we are using the same amount of crosslinker, but, when increasing the polymeric content, the network becomes less compact and will swell more. Matyash et.al. also saw a similar behavior regarding the crosslinking concentration in solution, stating the swelling increases with the decrease of CaCl2. [65] Gajic et.al. also state that, for the same crosslinking concentration, a higher polymeric content will increase the water retaining capacity. [66] On the other hand, hydrogels with the LMW alginate crosslinked with calcium did not present the same level of stability as the hydrogels with HMW. They started swelling in the first hours, but after 4 hours it is already possible to see the hydrogels losing weight and starting to dissolve

in the media. The smaller size of the polymeric chains, and the ionic bonds being less concentrated given the increase in polymeric content, makes the hydrogel brittle, this was also observable in the compression experiments, where the gels would start breaking as soon as the test started, splitting into small pieces. The large amount of polymeric content most likely forms a network with a lot of entanglement between the polymeric chains, which are physical interactions, easy to break. The LMW hydrogels crosslinked with calcium do not have stability in media, resulting in breaking and dissolving after a short period of hours. The loss of mass can also be attributed to the drying process performed before each weighting, that was done by carefully removing the hydrogels from the well-plate and placing them on a piece of paper. Sometimes small pieces of the hydrogel would break and stay in the piece of paper. The drying process was necessary to ensure that the weight being measured was just the mass of the hydrogel and its content, and not the media around it.

To know which polymer concentration was going to be used for the LMW oxidized alginate, several were experimented, crosslinked only with hydrazone bonds (Figure 3.3).

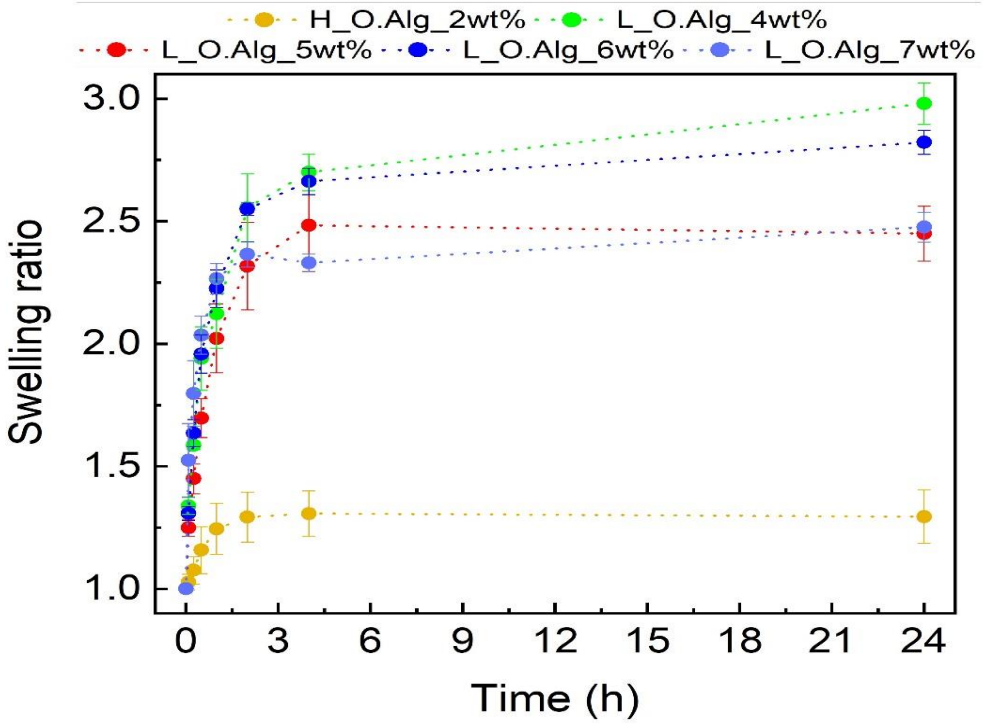

Figure 3.3 - Swelling graph of oxidized alginate crosslinked only with hydrazone bonds. In yellow is the hydrogels made with the High Molecular Weight alginate and the other samples were made with the Low Molecular Weight alginate varying the polymeric content.

Analyzing the graph, it is noticeable the difference in swelling between the LMW and HMW oxidized alginate hydrogels. The reason for this is either the different molecular weight or the higher polymer concentrations that allowed the hydrogels to uptake more water. However, when comparing only the LMW hydrogels with different polymer concentrations, it is seen that the swelling does not follow any type of trend when increasing the polymeric content of the hydrogels. Therefore, the swelling does not seem to depend on the polymer concentration for these hydrogels, which is probably due to the constant crosslinking degree.

After deciding on the 5 wt% polymer concentration, for the LMW oxidized alginate hydrogels, because of handling, and stability during the experiment. The influence of the crosslinking ratio on the swelling was then analyzed, and the results are shown in Figure 3.4. When the hydrogels were crosslinked only by hydrazone bonds, the swelling ratio is higher, but as soon as oxime bonds are added to the network, the hydrogels start swelling less. A clear trend can be observed when increasing the oxime bonds concentration - the swelling ratio decreases in the LMW hydrogels. A similar behavior is seen on the HMW hydrogels, even though only two different crosslinking ratios were evaluated. When the oxime bonds concentration is increased, the swelling decreases significantly. Morgan et.al. studied these same hydrogels using the HMW alginate, also observing a decrease in swelling when oxime bonds increased related to hydrazone bonds. [30] This is attributed to oxime bonds being stronger than hydrazone bonds. The hydrogel that presented less swelling was the hydrogel synthetized with the 40% oxidized alginate. Since there are more binding sites available for crosslinking, a higher crosslinking concentration is used to form the gel. This hydrogel was crosslinked only with hydrazone bonds, so the decrease in swelling can most likely only be attributed to the higher crosslinking concentration. A water-reuptake experiment was conducted on the freeze-dried hydrogels, to analyze their capability of retaining their structure after being freeze-dried. Most of the dry gels dissolved after roughly 12h submerged in PBS. The freeze-dried hydrogels that had been crosslinked with oxime bonds could maintain their structure up until 72h, but their initial properties were lost after the water re-uptake.

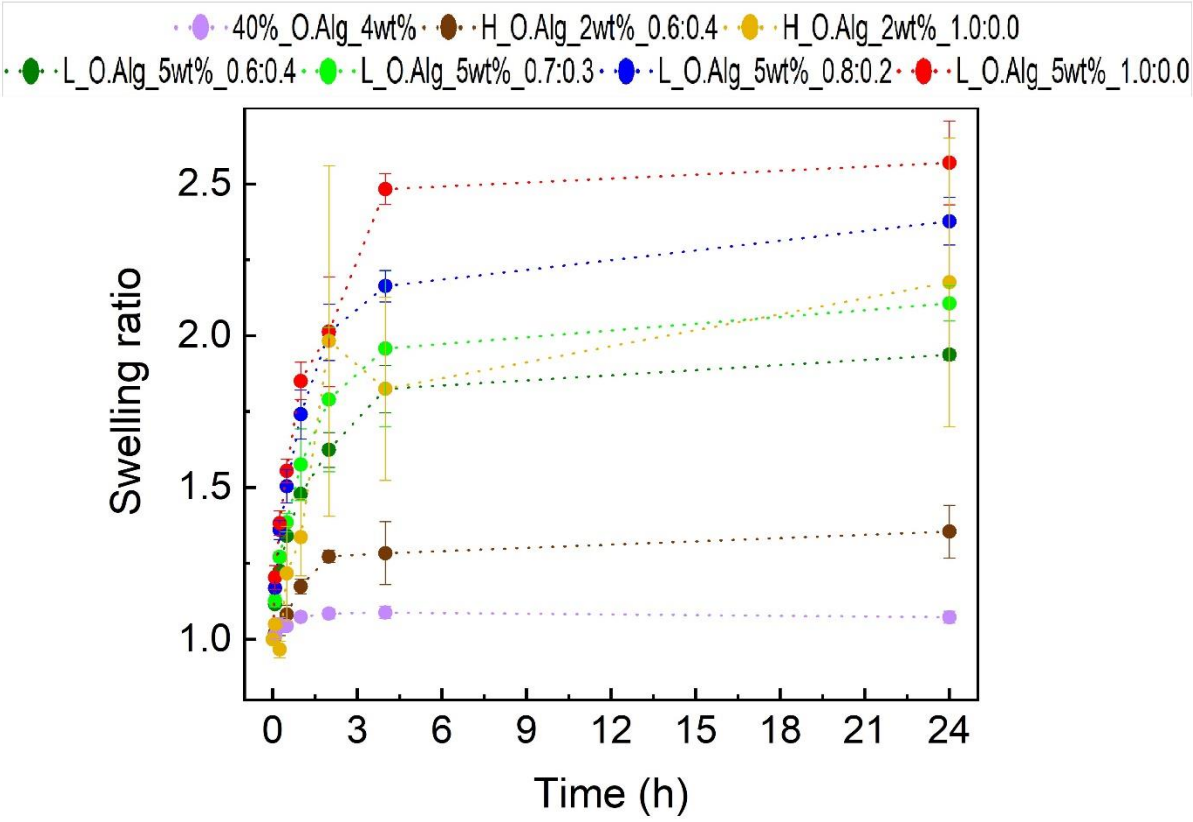

Figure 3.4 - Swelling of the oxidized alginate hydrogels with different crosslinking ratios (hydrazone:oxime), represented in light purple is the hydrogel with a higher crosslinking density (40%). The other hydrogels have a crosslinking of 10% of moles of alginate present in the hydrogel.

3.3 Porosity

The porosity of the hydrogels is a useful parameter to consider owing to their application for cell culture. The porosity graphs displayed in Figure 3.5 show values lower than what was expected. The expected values of porosity for these hydrogels would round values of 90% or similar, because of the low polymeric concentration in the hydrogels. However, the values obtained are lower than expected, probably the structure of hydrogels collapsed during freeze-drying step. For the alginate hydrogels crosslinked with calcium, the porosity obtained for the LMW hydrogel was higher than the porosity obtained for the HMW. However, considering the error bars, it is possible to say that the porosity values are not significantly different. As for the oxidized alginate hydrogels, more formulations of hydrogels were assessed. They have porosity values similar to each other. Looking only at the LMW hydrogels, there seems to be a trend regarding the ratio of crosslinker. With a higher oxime concentration, the porosity looks like it decreases, except for the 5wt% 0.7:0.3 hydrogel, which has a bigger error bar than the other

samples. Nonetheless, this possible trend might be related to the stronger oxime bonds creating a more compressed network. However, this trend does not happen on the HMW hydrogels, but the standard deviation for the 2wt% 0.6:0.4 is noticeably high, which might be why this trend is not seen on the HMW hydrogels. Also, only two formulations were tried with the HMW alginate, so it is hard to even assume any type of trends.

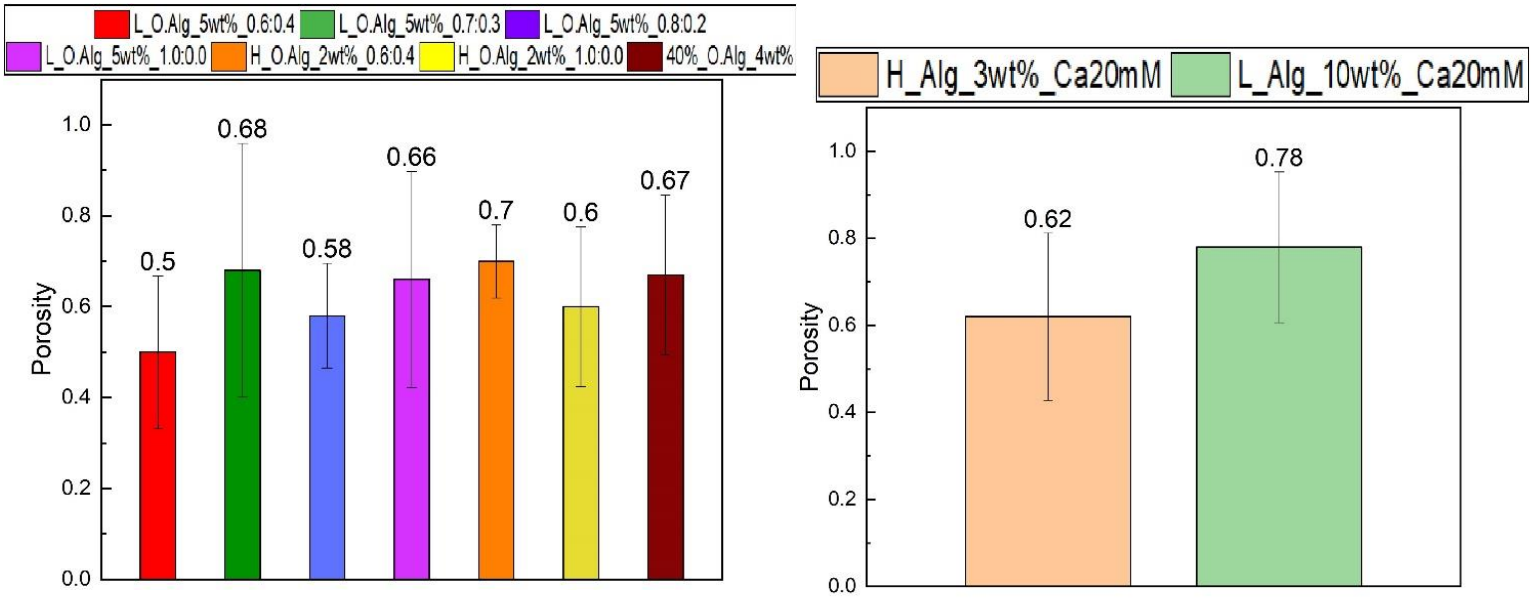

Figure 3.5 - Porosity, to the left are represented the obtained porosity values for the oxidized alginate hydrogels, and to the right the porosity of the hydrogels of alginate crosslinked with calcium.

3.3.1 SEM

The hydrogels formulations used for cell experiments were also freeze-dried and imaged in the Scanning Electron Microscope (SEM). The SEM images, Figure 3.6, were useful to correlate with the porosity values obtained in the prior experiment. The porosity values obtained show that the porosity values for the different hydrogels' formulations are similar to each other, which is confirmed by the SEM pictures. With this imaging, it was possible to see that the different hydrogels have a remarkably similar structure, and pore sizes around the same values when dried (ranging from 60μm to 150 μm). The 2wt% 1.0:0.0 hydrogel and the 3wt% 20mM pictures look different to the other ones, which was associated with the wear down of the two samples used.

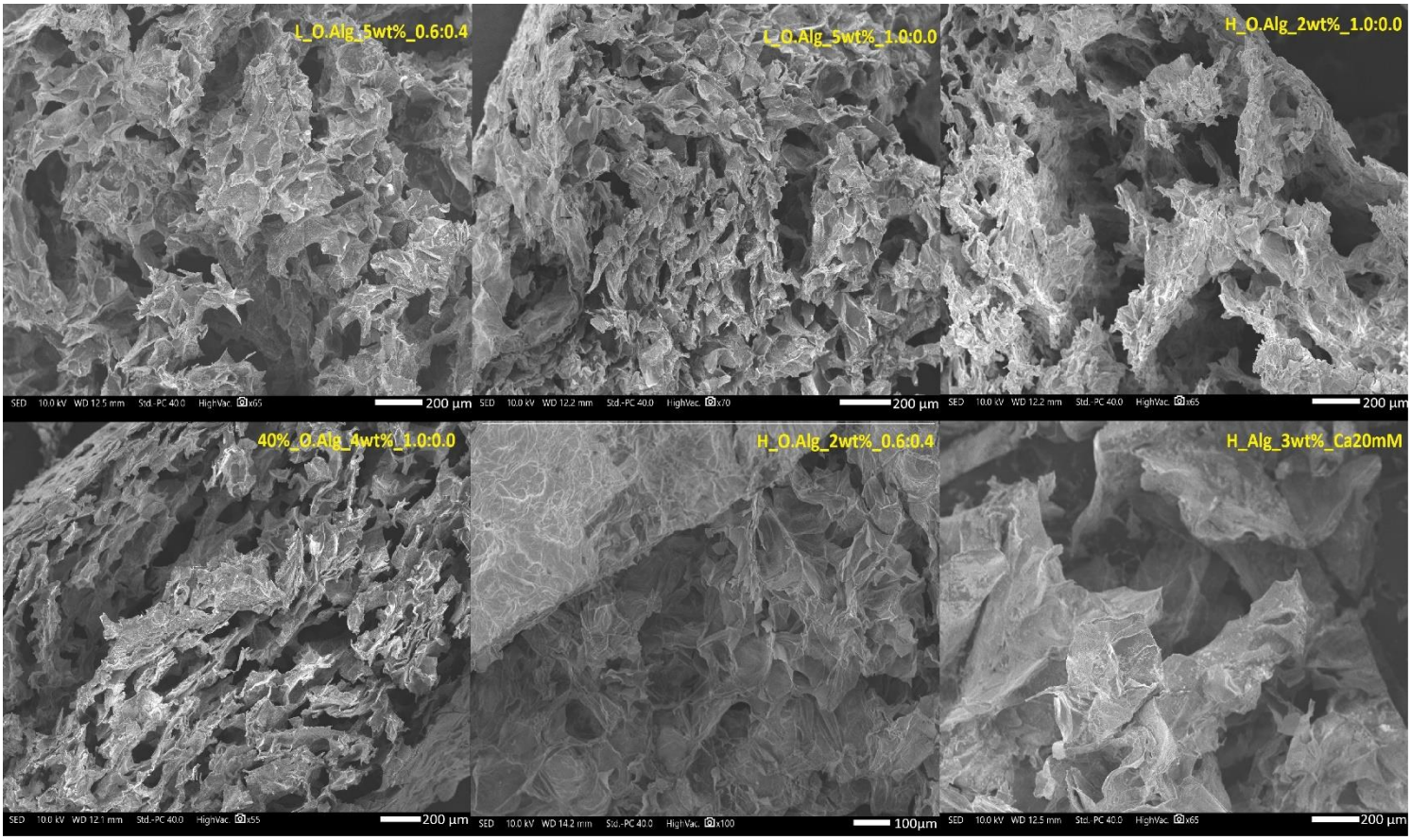

Figure 3.6 - SEM images of the dried hydrogels with the formulations that were used for cell experiments.

3.4 Compression

Mechanical compression testing was done with the hydrogels in two different conditions: before and after swelling in culture media, aiming to compare the mechanical properties.

The ultimate compression stress of the hydrogels before failure, and the Young Modulus (Compression Modulus) were determined, which allows us to evaluate the hydrogel stiffness along the different formulations. The Young Modulus can be tricky to calculate in hydrogels, especially for very soft ones given that it is hard to understand where the linear area of these graphs starts and ends (Compression graph, D in supplementary information). Therefore, the calculation of the Young modulus is made by analyzing the slope of the strain/stress curve, in the early instances of deformation (usually from 5% to 15% strain). This was the region used for the hydrogel with 40% oxidation, because it was more brittle and stiffer than the other ones. For the other hydrogels, since they were very soft, the region chosen to obtain the Young

Modulus was 10-20% strain, because the values fitted the slope well. Also, that strain percentage ensures there is considerable stress being applied to the hydrogels.

The hydrogels crosslinked with calcium were breaking constantly during the compression (not deforming but breaking over time), this was associated with fact that ionic bonds are weaker (compared to covalent bonds) and therefore the calcium hydrogels could not retain their structure during the experiment. Moreover, because alginate gelates very fast with calcium, putting them in the mold sometimes required to break them. Even though the ionic crosslinking can self-heal the hydrogels, and that the gels were left in the mold for 24 h before use, some fissures could still be present. Because of this, the ultimate compression stress of these hydrogels was not analyzed since they were not keeping their structure from the start of the experiment, both before and after swelling. On the other hand, the oxidized alginate hydrogels (11% theoretical oxidation) were able to withstand stress up to 60-120 kPa, depending on the crosslinking ratio and the polymeric content. It looks like there might be a trend associated with the ratio of crosslinkers used for the ultimate compression stress, but this is hard to confirm. When the hydrogels are only crosslinked with hydrazone bonds, they are able to deform more before rupture. For the hydrogels crosslinked also with oxime bonds, they cannot deform as much due to these stronger bonds. The ultimate compression stress does not seem to depend on the type of crosslinker, for the oxidized alginate hydrogels, Figure 3.7, because after statistical analysis the difference in the values are not significant for $p \leq 0.05$. When increasing the polymeric content, the trend seems to indicate that the ultimate compression stress decreases. However, the difference in values is not significant for $p \leq 0.05$. The ultimate compression after swelling decreased for all the samples. All of them, except for the 5wt%0.6:0.4 (LMW) hydrogel, have a similar value. The hypothesis for this not happening in the mentioned hydrogel is the number of oxime bonds. When there are enough oxime bonds present in the network and the hydrogels have a higher polymeric content, it looks like it can maintain its resistance to stress better.

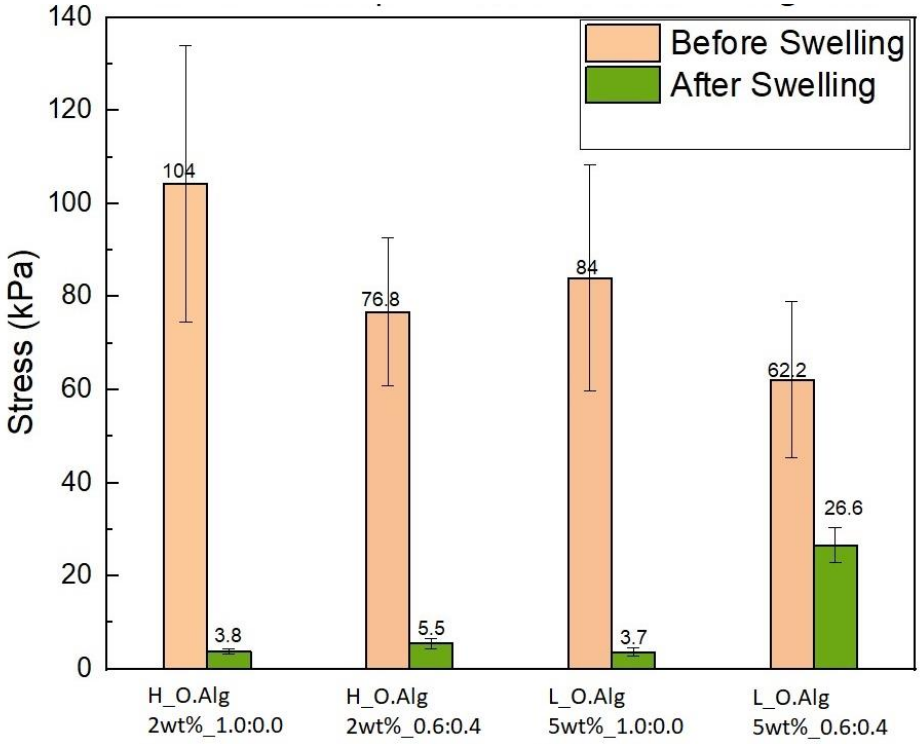

Figure 3.7 - Ultimate Compression Stress of the oxidized alginate hydrogels both high and low molecular weight, with two different crosslinking ratios.

Figure 3.8 displays the values obtained for the Young Modulus of the different hydrogels. The hydrogels crosslinked with calcium seem to have their young modulus increased with the increase in polymeric content. The data obtained from the oxidized alginate hydrogels, on the other hand, allow us to see an increase in young modulus associated with the increase in polymeric content, which is likely associated with the higher entanglement of polymeric chains that comprise the hydrogel network. The results show the influence of the oxime bonds in the Young modulus of these hydrogels. As soon as oxime bonds are added to the network, the Young modulus increases for both the high molecular weight and the low molecular weight hydrogels. This was expected because of how stronger the oxime bonds are compared to the hydrazone bonds. The hydrogel synthesized with the 40% oxidized alginate also presented a higher young modulus than the other hydrogels crosslinked only with hydrazone bonds. This was associated with the higher crosslinking sites present in the hydrogels, resulting in a stiffer gel.

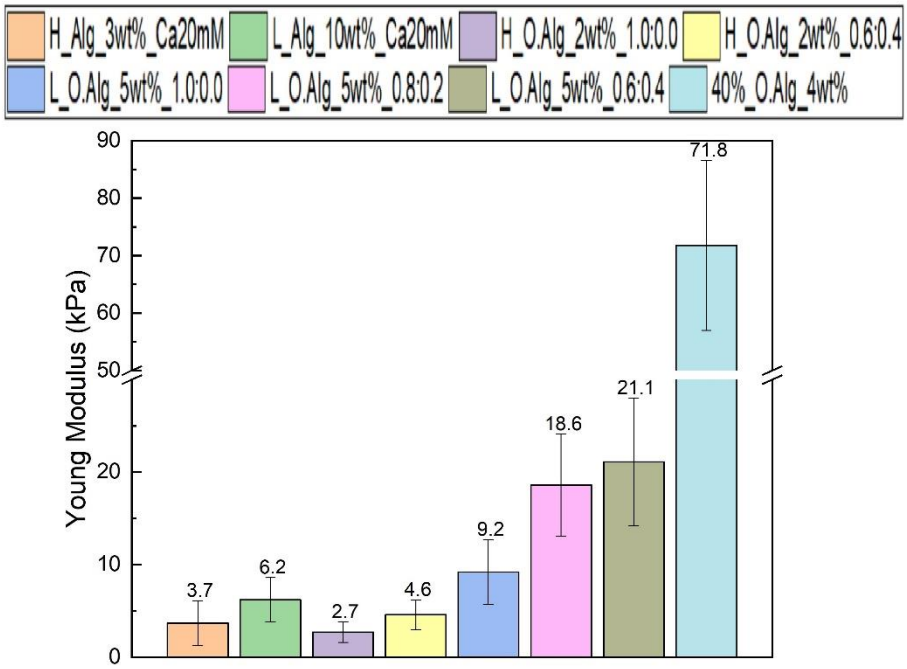

Figure 3.8 - Young Modulus obtained for the different hydrogels made with alginate and oxidized alginate.

Figure 3.9 shows the Young Modulus after swelling. It changes significantly for some samples, but not for others. Nonetheless, it is curious that hydrogels with oxime bonds might have had their young modulus increased slightly, the values obtained for the hydrogels crosslinked with oxime bonds show the Young Modulus increased significantly in a statistical analysis for $p \leq 0.05$. On the other side, for the hydrogels with only hydrazone bonds, a slight decrease in the average values can be seen. For the 5wt%1.0:0.0, the decrease is significant for $p \leq 0.05$, but the decrease for the 2wt%1.0:0.0 was not significant for the same p-value. Therefore, it is not possible to conclude if the Young modulus of the hydrogels actually decreases after swelling because of the behavior not being significant for both of these samples. However, for the hydrogels with oxime bonds, the increase in young modulus seems to be significant for $p \leq 0.05$. It was hypothesized that it is associated with crosslinking, which creates a more compressed network. When the hydrogel is fully swollen, the presence of these stronger bonds makes the hydrogels slightly stiffer, while the hydrazone bonds do not have the strength to create the same tension in the network. The alginate hydrogels crosslinked with calcium ions show different results. While for the 3wt%20mM (HMW) the young modulus seems to increase, for the other hydrogel, 10wt%20mM (LMW), the young modulus decreased. For the 3wt% (HMW) sample the difference is not significant for $p \leq 0.05$, while it is significant for the 10wt% (LMW)

for p≤0.05. However, it is not possible to know from this data if this behavior would always happen, since there are still big errors associated with the values.

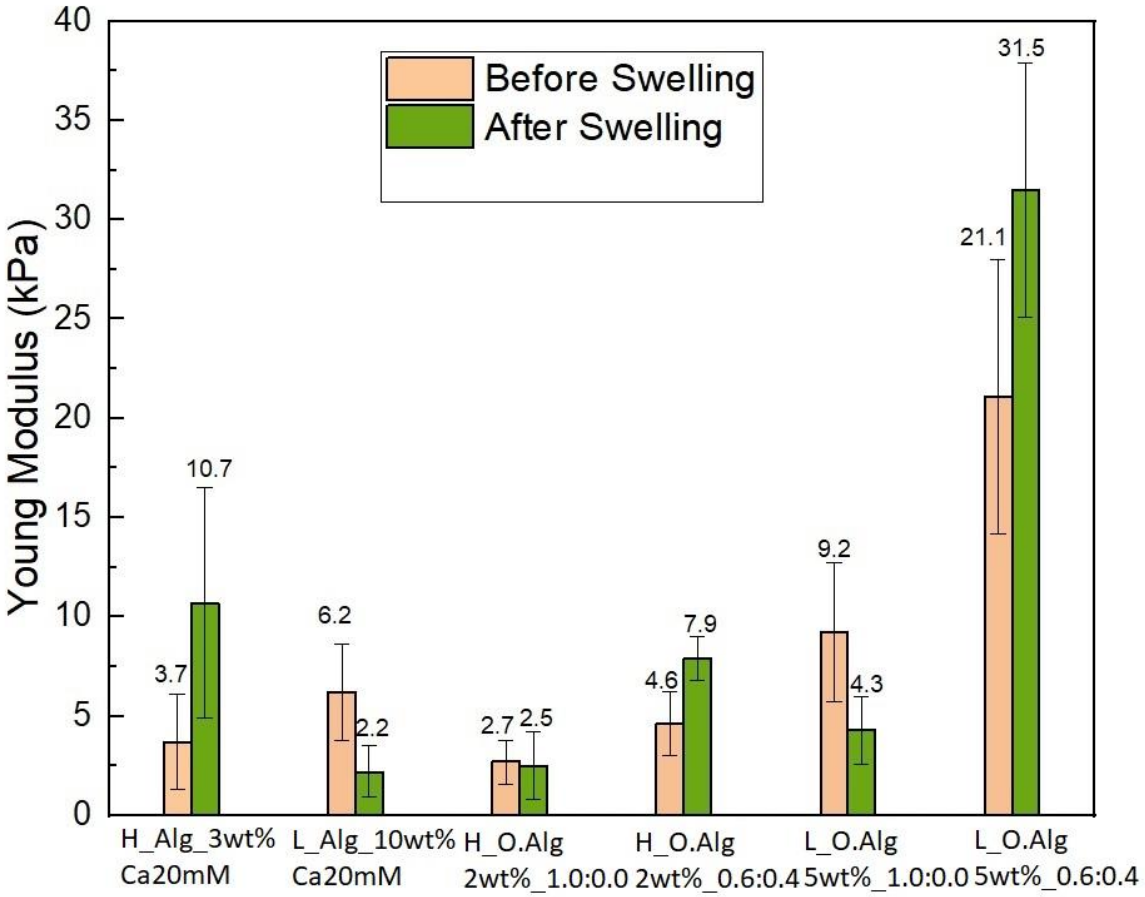

Figure 3.9 - Young Modulus of the different hydrogels (high and low molecular weight) before and after swelling in media for 24h.

3.5 Stress-relaxation

Stress-relaxation is the decrease in stress under a constant strain, which is evaluated according to the time it takes for the tissue or material that is being analyzed to relax. It was an important experiment to perform given that some papers have previously stated that faster relaxing materials improved neurogenesis. [5,29] Moreover, it is interesting to compare the values obtained to the time of stress-relaxation of native tissues, even though the experiments have not been performed on the hydrogels and the native tissues using the same protocols. The value that is going to be used to characterize the samples is the time for half-relaxation. Comparing the different samples (Figure 3.10), there is a clear influence of the crosslinker in the time for half-relaxation. This behavior is in accordance with a previous work by Morgan, *et al.* which

reported the lower pK_a crosslinker presents a faster stress relaxation. The adipic dihydrazide that forms hydrazone bonds has a reported pK_a of 2.5, while O-ethylhydroxylamine (representative molecule of the *O*, *O'*-1,3-propanediylbishydroxylamine dihydrochloride, the molecule used to form the oxime bonds), has a reported pK_a of 4.65. [30]

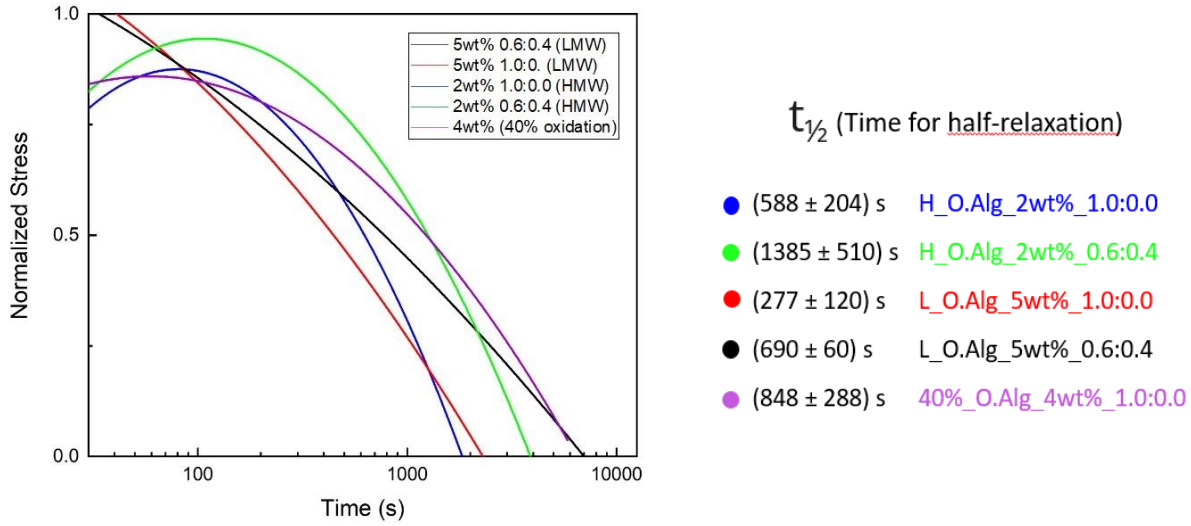

Figure 3.10 - Trend line of the stress-relaxation graphs obtained for the different oxidized alginate hydrogels made. Also represented in the image are the half-time relaxation for the hydrogels.

The impact of the addition of oxime bonds has been shown by Morgan, *et al.* where in the paper it is clearly demonstrated the increase in the half-relaxation time by the addition of oxime bonds to the network. [30] The polymeric content in the hydrogel also seems to have an influence in the relaxation time. The bigger presence (in number) of binding sites possibly allows the dynamic crosslinkers to find binding sites more easily and more quickly attaching, leading to a faster stress-relaxation time. Moreover, Chaudhuri, *et al.* were able to modulate the stress-relaxation of alginate hydrogels, by changing the molecular weight of the alginate used to synthesize the hydrogel. [67] Since in this case the concentration of polymer and the molecular weight of the polymer is changing, it is difficult to know which of these has a bigger impact on the stress-relaxation. But this statement can only be used to do a comparison of the alginates that were oxidized and crosslinked to a concentration of 10% of the mols of alginate present in the hydrogel. Looking at the alginate that was oxidized up to 40% and crosslinked only with hydrazone bonds, the higher crosslinking density seems to slow down the relaxation process. This is possibly associated with the higher percentage of bonds that need to be reattached after the application of stress to recover the initial state. The increase in crosslinking density leads to a more compact network, less susceptible to deformation, in opposition to the other hydrogels.

The time for half-relaxation of the alginate hydrogels crosslinked with calcium were not considered to be accurate results, Figure 3.11. During the experience, what was happening was that, after the maximum strain applied was reached, the hydrogel would also hit the point of maximum stress, but then almost immediately break due to the weaker ionic bonds that cross-link the hydrogels. After the first minutes of the experiment, it is possible to observe from the graphs that the hydrogels slow down their relaxation a lot and only reach full relaxation by the same time as the other hydrogels. (After the 1000s time point)

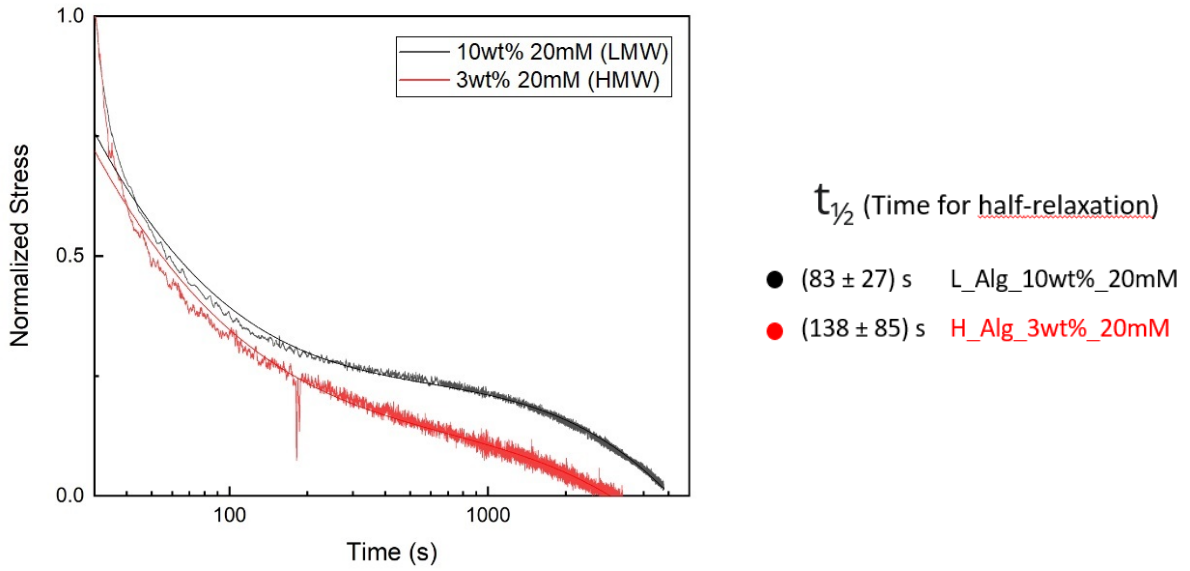

Figure 3.11 - Stress-relaxation graphs, and trend line obtained for the alginate hydrogels crosslinked with calcium. Also represented in the image are the half-time relaxation for the hydrogels.

The whole experiment was not performed with the best conditions, since the machine utilized to assess the stress relaxation was not placed on a proper table to avoid big vibrations. Therefore, a lot of variation can be seen on the data. (D in supplementary information) Also, loud noises would influence the values obtained due to the big sensibility of the load cell being used. Moreover, there was nothing covering the sample during the three-hour experiment, so the only approach the machine allowed to avoid water evaporation during the long experiment was to carefully place water around the hydrogel. The big errors associated with the values can also be justified by the difficulty that existed in making hydrogels that were all exactly the same size and with a flat and constant contact area, which ended up causing variations between samples. The stress-relaxation assays are usually not performed on a mechanical tester, especially for soft hydrogels that make it hard to have a clear signal. However, at the time it was what was available to perform the experiment, and it allowed to take conclusions comparing

the different hydrogels tested. It would be interesting to try doing the stress-relaxation on a properly set-up rheometer to compare the values.

3.6 Cell experiments

Using the different hydrogels formulations mentioned in 3.5 (stress-relaxation), cell experiments were performed. Two different cell types were used in these experiments: iPCS differentiated into nociceptors spheroids, and PC12's. Initially, the cultures were being maintained for a period of seven days, but due to the instability of the hydrogels in culture, the culture time was reduced. The hydrogel formulations experimented with for each cell type is represented on table 1 for the nerve spheroids and table 2 for the PC12's. The main difference between the two tables is the replacement of the L_Alg_10wt%_Ca20mM hydrogel for the 40%_O.Alg_4wt%_1.0:0.0. The hydrogel was replaced because it was too opaque given its high polymeric content which difficulted imaging. The 40% oxidized alginate hydrogel was added to the experiments to assess the influence of higher crosslinking ratio in the stability over time in culture.

Table 1 - Hydrogel formulations used to seed the nerve spheroids.

H_Alg_3wt%_Ca20mM	H_O.Alg_2wt%_1.0:0.0	H_O.Alg_2wt%_0.6:0.4
L_Alg_10wt%_Ca20mM	L_O.Alg_5wt%_1.0:0.0	L_Olg_5wt%_0.6:0.4

Table 2 - Hydrogels formulations used to seed the PC12 cells.

H_Alg_3wt%_Ca20mM	H_O.Alg_2wt%_1.0:0.0	H_O.Alg_2wt%_0.6:0.4
40%_O.Alg_4wt%_1.0.0.0	L_O.Alg_5wt%_1.0:0.0	L_Olg_5wt%_0.6:0.4

3.6.1 Culture strategies

Human iPCS differentiated into nociceptors spheroids, with a diameter of around two hundred µm were the initial cells being used in this project. Usually per well 5 to 10 spheroids would be added to the each well, because it was observed that less than that makes it difficult to find them in the microscope. Different approaches were conducted with the objective of creating the best possible conditions for the cell culture in the alginate hydrogels. In the first experiment, conducted in alginate hydrogels crosslinked with calcium, two approaches were tested: dispensing a suspension of cell spheroids on the surface of the hydrogel (2D), and seeding the spheroids inside of the hydrogel by opening the hydrogel with the pipette tip and placing them inside. The main difference between this 2D and 3D approach is that in 2D the spheroids are placed on top of the hydrogel and do not move inside, on the 3D approach by breaking open the hydrogel and placing the spheroids inside it is possible to ensure that the spheroids are surrounded by the alginate hydrogel.

Positive results were achieved from the 3D experience, and pictures taken during culture can be seen in Figure 3.12, where it is possible to observe axons growing from the nerve spheroid. The spheroids seeded using the 2D approach did not demonstrate any type of axon growth. Given the positive results obtained in the 3D experience, and since it is more interesting to be able to create a 3D environment to grow the nerve cells, the 2D approach was abandoned.

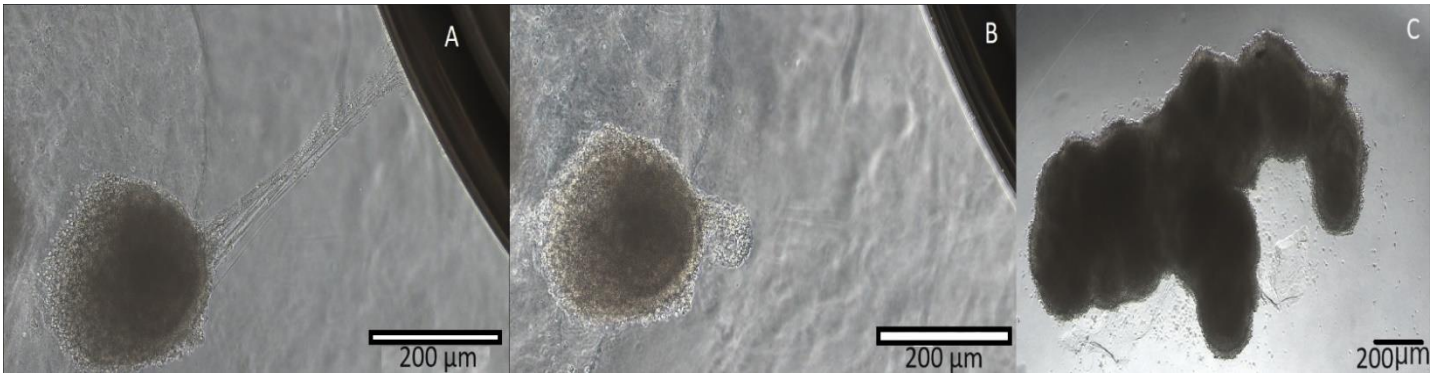

Figure 3.12 - Picture taken of a nerve spheroid in brightfield in alginate hydrogels crosslinked with calcium (H_3wt%_20mMCa) A -picture taken at the 6th day of culture, it can be seen a long axon growing out of the nerve spheroid. In this picture the strategy used was the 3D approach mentioned. B- Retracted axon after breaking on the next day. C- Image taken also on the 6th day of culture, but on the 2D approach, the cells clustered and did not show signs of growing axons.

A new problem arose with the oxidized alginate hydrogels: because of the swelling of these gels and the smaller polymeric chains, the hydrogels were more prone to dissolve during culture. Because of this, the strategy of breaking the hydrogels and inserting the cells directly inside did not suffice, since the hydrogels more easily dissolve if broken into smaller pieces. The hydrogel dissolution would then lead the cells to be in suspension, and not in contact with the hydrogels, which was the objective. Therefore, to ensure that the cell spheroids were growing in 3D and that they were always in contact with the hydrogels, a new method of encapsulation was used by making a hydrogel sandwich. The hydrogels were prepared in a sterile 96-wellplate, with the spheroids placed on top of one of the hydrogels. Another hydrogel with the same properties was placed on top to create a hydrogel structure with the cells seeded in the middle. The strategies used for culture are demonstrated in Figure 3.13.

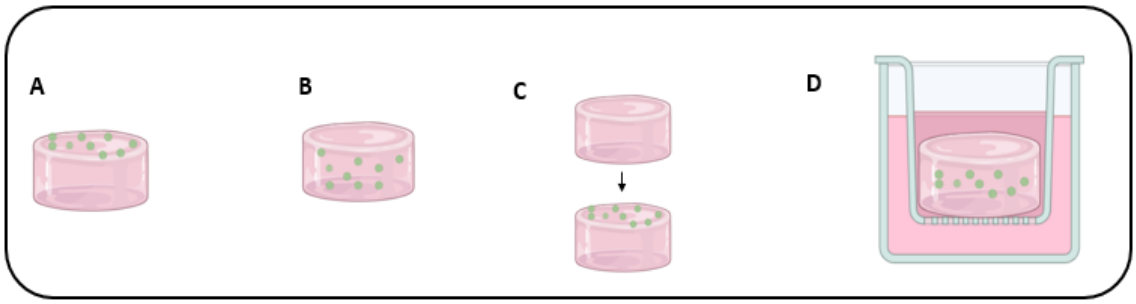

Figure 3.13 - Strategies for cell culture. A- 2D culture; B-3D culture; C- 3D-sandwich; D- culture with a transwell. Image created in biorender

Problems that must be remarked when using this method: first, the hydrogels cannot be too tall, or else they will difficult imaging due to the microscopes' working distance. This problem gets worse when the hydrogels start swelling, which then does not allow clear pictures of the cells; secondly, placing two hydrogels in the same culture well creates challenges to perform media changes. The hydrogels occupy a lot of space, and after they swell it becomes even more problematic. In some cases, it was not possible to properly remove and add new media to the culture. Moreover, on account of the space they occupied, it was hard to perform the media without touching the hydrogels and disturbing the cells, which is a problem given they grow attached to the substrate. This problem was a major priority since the objective was for the cells to grow axons, and given that they are very fragile, if they are disturbed it is likely that the axons will end up breaking. With this said, one later approach was to use well inserts to avoid contact of the pipette tip with the hydrogels, so the cells would not be disturbed. This did not resolve the problem with the microscope working distance, so the images captured were still blurry. A problem that arose from using the well inserts was hydrogel dissolution, by increasing

the ratio volume of media and volume of hydrogel, the hydrogels started to dissolve more rapidly. After 5 days, the cells were fixed and, when doing the staining, it was noticeable that the hydrogels had completely dissolved, which would not happen prior to using the well inserts.

The results obtained are going to be discussed further in the thesis, but as a consequence of the problems mentioned, it was decided to change the cells that were being used and start using the PC12 cell line. The objective of using these cells was to simplify a bit the culture process, with smaller cells that can also survive and grow more easily.

The culture and priming of the PC12 cells have already been described in the Materials and Methods section. After the priming, the cells are detached and deposited on top of the hydrogels that were already formed at the bottom of the well. To improve the working distance problem, the thickness of the hydrogels was reduced (less volume used to prepare the gels). The smaller size of these cells (around 20μm) compared to the spheroids (around 200 μm) also allowed them to penetrate inside the hydrogels more easily, without the need for adding an extra hydrogel on top, to ensure the cells were fully surrounded by hydrogel.

3.6.2 Microscopy

Fluorescent imaging was used to analyze the axon growth on the nerve spheroids, using phalloidin to stain the F-actin cytoskeleton of the cells, and DAPI to stain the nucleus. Some brightfield images were also taken during culture when axons were observed. Across the different experiments made with cells, one thing was noticeable in all of them. Even when axon growth had been visualized, after media changes and staining procedures axons were no longer observed. In some cases, it was possible to see a retracted axon, which is a consequence of axons breaking or loss of their attaching point (Figure 3.12). Hydrogel stability proved to be crucial for axon growth, since it is associated with the attachment of both the growth cone, and cell body to the hydrogel. Initially, the cells were kept in culture over a period of 7 days and then the culture period was reduced to 4 days to avoid the hydrogels degradation and its influence in cell development. Moreover, the results from the first culture showed that axon growth would be possible within this reduced period. However, afterwards, it was not possible to see by fluorescent imaging axons growing out of the neuron spheroids cultured for 4-days. The images show a lot of cells surrounding the spheroids, possibly dead cells. It was hypothesized that they forced out of the spheroid formation by the viable cells (Figure 3.14).

Furthermore, the brightfield images show strange structures, that do not appear in the fluorescence images, even when the cells are over exposed to light. Since bacteria and fungi

usually appear in fluorescence, these structures were associated to hydrogel degradation (Figure 3.15).

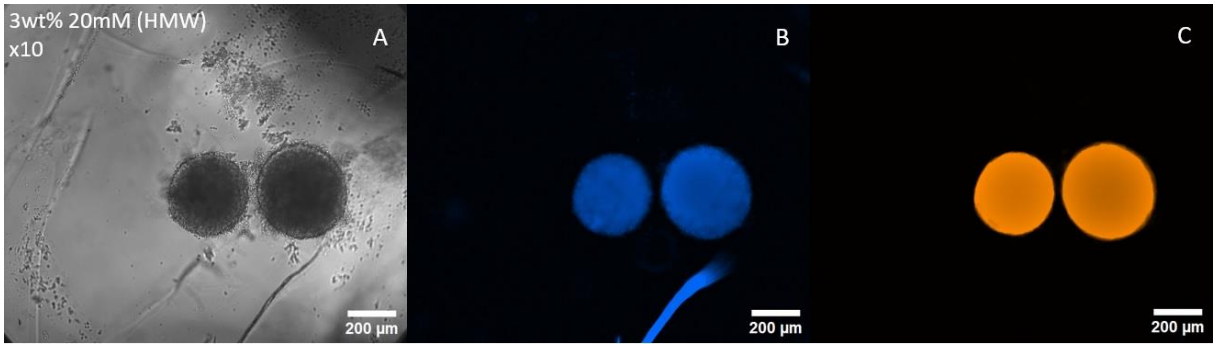

Figure 3.14 - Image of nerve spheroids expelling cells. A-Brightfield; B-DAPI; C-Phalloidin.

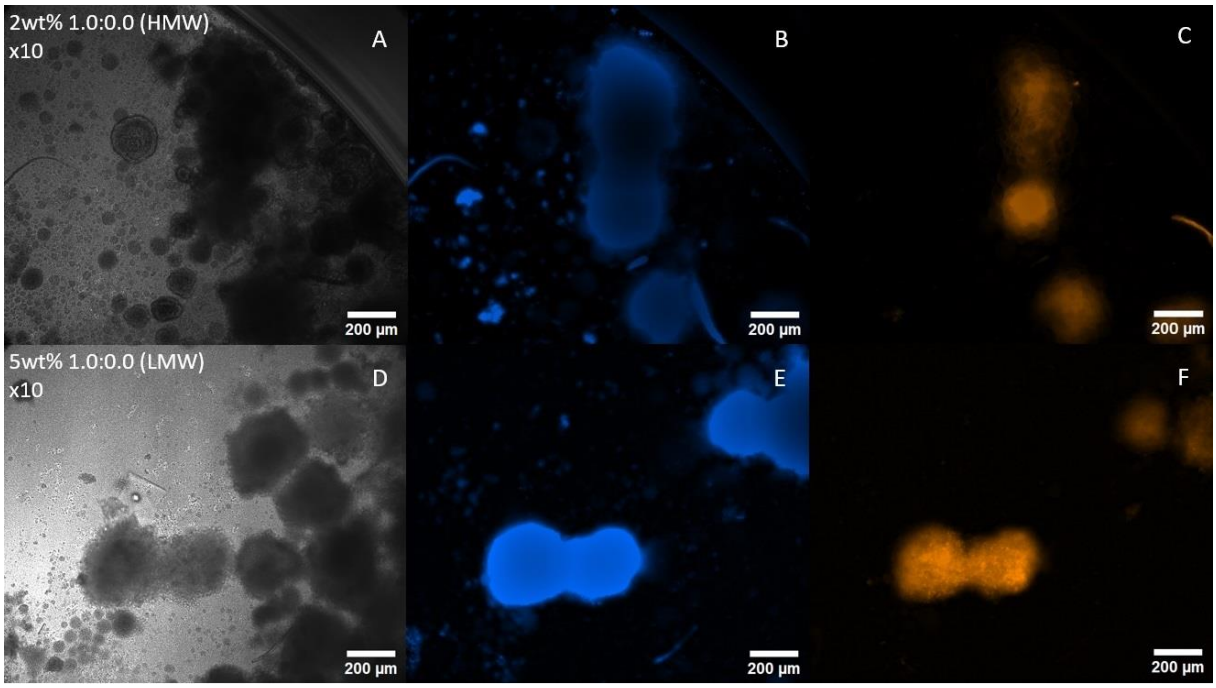

Figure 3.15 - Strange structures that appeared in culture. 1st line is a picture taken after fixing the cells in the hydrogel with the formulation H_O.Alg_2wt%_1.0:0.0 A-Brightfield; B-DAPI; C-Phalloidin, D-Brightfield; E-DAPI; F-Phalloidin.

A lot of pictures taken in the different samples used show that the cells were most likely dying and were probably not adapting to the culture environment. This might happen because of the lack of stability of the hydrogels, which start degrading and do not allow the cells to attach and grow. Also, if the cells can attach in the beginning and start growing axons, dethatching breaks the axons, and, after the axons break, it is very likely that the cells will die, due to cell damage. One other reason for the cells not being adapted to the environment is the swelling mentioned earlier that made the media changes hard, which might mean that the cells by the

end of the culture period were underfed and dying because of that. More pictures illustrating what was mentioned can be observed in B.1 in supplementary information.

Due to these problems, and since the results were not promising to move forward, the cells used were changed to PC12s'. These cells are smaller and easier to culture, and even though they are not present in the human body, they are accepted as a model to study all types of neurological diseases. Therefore, the possibility to create a 3D environment where neuron like cells (PC12's) can grow is interesting to maybe further ahead creating 3D models of neurological diseases. Because of the smaller size, it was easier to ensure the cells would penetrate the hydrogels, and it was possible to reduce the working distance. The PC12s' were stained with deep red cell tracker, the cell tracker passes through the membrane of cells and react with amine groups on proteins, so that images could be taken throughout all the culture days. For this, the LiveCell Imaging System was used, which allowed to place the wellplate inside an incubator for imaging. In some experiments done with these cells', fungi infections kept appearing, even though the hydrogels were placed under 265nm UV light for 5-10 minutes. Because of this, the solutions to prepare the hydrogels had to be filtrated through a 0.2 µm filter before hydrogel preparation, all inside a flow hood.

The first thing to understand in the culture was how many cells could be seeded in the hydrogel, because too many cells would create clusters, and they usually do not grow axons while in big clusters. In addition to that, if enough cells are not seeded, they end up dying. After experimenting and considering the work performed by Malheiro, *et al*. and the advised number by Thermo Fisher the number of cells per hydrogel in a 96-wellplate was found to be between 4000-5000 cells. [68] The cells were monitored, and pictures were taken, over 3 days in culture (Figures 3.16, 3.17 and 3.18). After 24h, it is already possible to see in regions of the hydrogels some cells that are starting to develop axons. In some of the most dynamic hydrogels (composed only of hydrazone bonds), it is possible to see clustering of cells over a very thin fissure. Considering the way hydrogels were prepared for these experiments (Inserting the hydrogel solution in the wells and leaving them to gel overnight), it is possible to hypothesize that those fissures, in Figure 3.16 (E, F, G, H), were created in the hydrogel by the cells themselves. These fissures are most likely being created because the dynamic network allows the cells to move more freely inside the hydrogel, permitting them to cluster and possibly find areas with greater stability, remodeling the structure of the hydrogel. When looking at the pictures with the fluorescence turned on, the cell tracker lights up on those fissures in the hydrogel. This was associated with the fact that, for the axons to properly be seen with the cell tracker, it was necessary to overexpose the image to fluorescent light, even in the control,

because the cell tracker did not have a very strong signal. Therefore, it is possible that those fissures are just reflecting light. However, this cannot be confirmed and one other theory that also might fit these images is that the cells are growing axons within those fissures. It was hypothesized that the cells may be moving and clustering into those regions, and being able to find stability areas where they can attach and grow axons along those lines that may employ more stability than the other regions of the hydrogel.

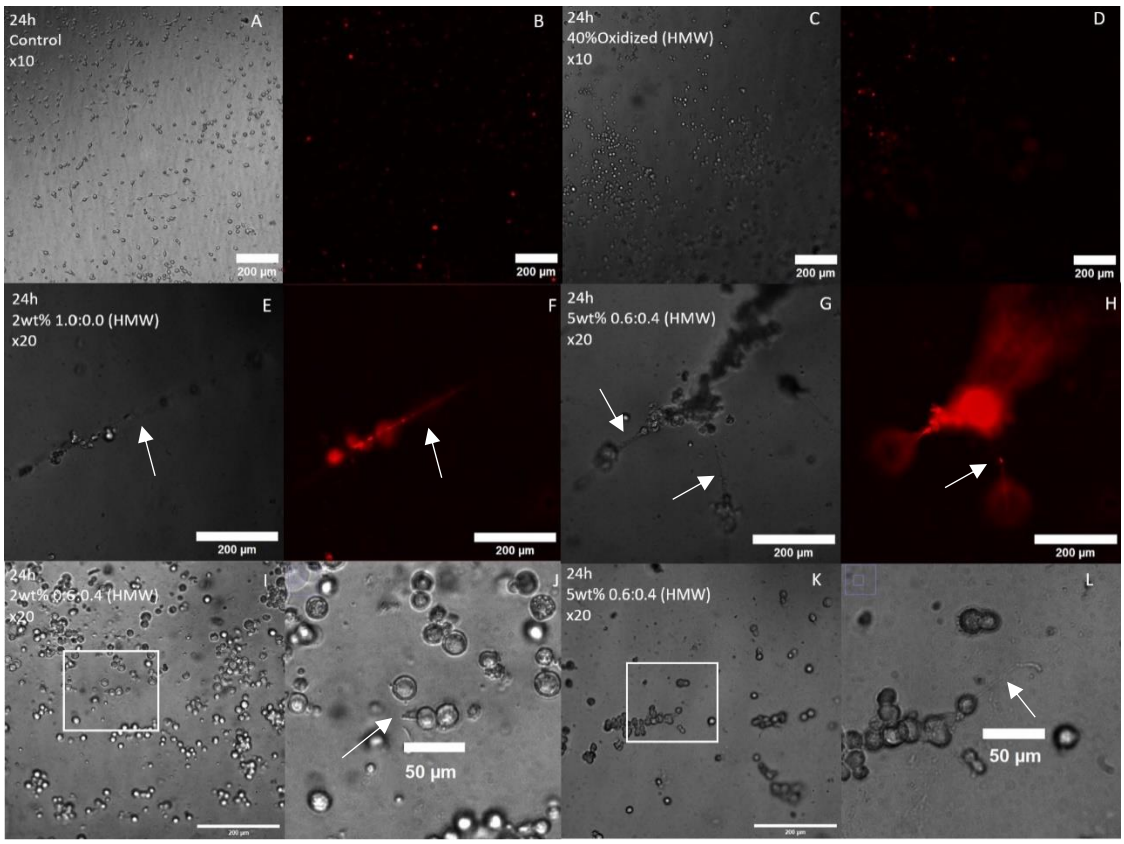

Figure 3.16 - Pictures taken after 24h of culture in the hydrogel. 1st line, Image A and B correspond to the control well (well coated with collagen) A- Control Brightfield; B- Cell tracker; 1st line C and D correspond to the hydrogel formulation 40%_O.Alg_4wt%_1.0:0.0 C- Brightfield, D- Cell tracker image of C; 2nd line E and F correspond to images taken in the hydrogel with the formulation H_O.Alg_2wt%_1.0:0.0 E-Brightfield; F- Cell tracker image of E; 2nd line G and H represent Images taken on the hydrogel with the formulation L_O.Alg_5wt%_0.6:0.4 G- Brightfield and H - cell tracker image of G. The fissures mentioned are pointed out by the arrows in the image. On the third-row image J and L are close up pictures of I and K that possibly show axons growing. pointed out by the arrows.

On the second day of culture more cells appeared to be growing axons, but it was not possible to confirm it with the cell tracker for most of the cases. Most of the pictures that (possibly) show axons were taken in the hydrogels with the LMW 5wt% 0.6:0.4 (hydrazone:oxime ratio), which was not expected given that other papers mention nerve cells would grow more in faster stress-relaxing environments, and softer materials, similar to the native brain. [5,26-29] This

was not what was seen in this project, and the main justification is the hydrogels' stability. Stronger bonds present in the network, and a higher polymeric content, may provide the hydrogels with areas of stability for the cells to grow. On the hydrogel crosslinked only with hydrazone bonds there are pictures that possibly show axons (Figure 3.17 I and J), but they look a bit deteriorated, possibly due to the lack of stability over time. Figure 3.17 shows some of the pictures taken during culture on the second day. More can be seen on B.2 in supplementary data.

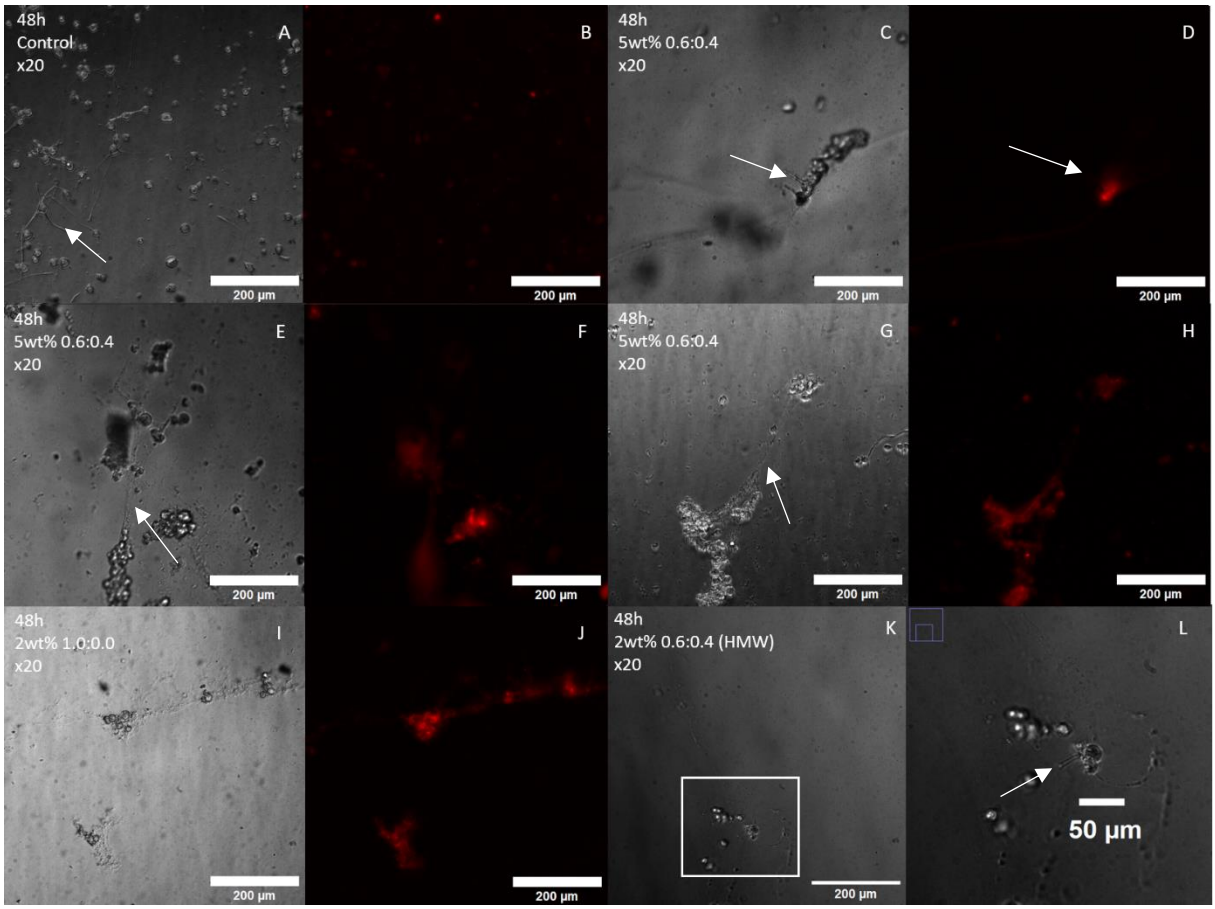

Figure 3.17 - Pictures taken after 48h of cell culture in hydrogels. A and B represent the control culture well (collagen coated well; C, D, E, F, G, and H correspond to pictures taken in the hydrogel with the formulation L_O.Alg_5wt%_0.6:0.4. C- Brightfield; D cell tracker image of C; E- Brightfield; F- Cell tracker image of E; G-Brightfield; H cell tracker image of H; I and J are pictures taken on the hydrogel with the formulation H_O.Alg._2wt%_1.0:0.0; I-Brightfield; J cell tracker image of I; image K was taken on the hydrogel with the formulation H_O.Alg._2wt%_0.6:0.4 and L is a close up picture of K. The arrows in the picture point to what is thought to possible be axons.

By the third day of culture, barely any axons could be seen, even in the control wells. As mentioned before, the hydrogels with the 5wt%0.6:0.4 formulation were the ones that showed more axons, comparing to the other formulations, but by the third day less cells could be found in the hydrogels (Figure 3.18). This was possibly due to the media change that was done after the

imaging, which could have washed away unattached cells which are unattached due to hydrogel degradation throughout the days in culture. No degradation tests were performed in the hydrogels to quantitatively access the degradation. For example, rheology measurements could have been done in different time points to access the loss of properties over time. [69] Because of the differences in the cells observed from the second to the third day, by the fourth day a life/dead assay using Hoechst (Blue, label all live and dead cells) and Propidium Iodide (Yellow, label dead cells only) was performed because it seemed necessary to understand if the cells were dying or if they were just washed away.

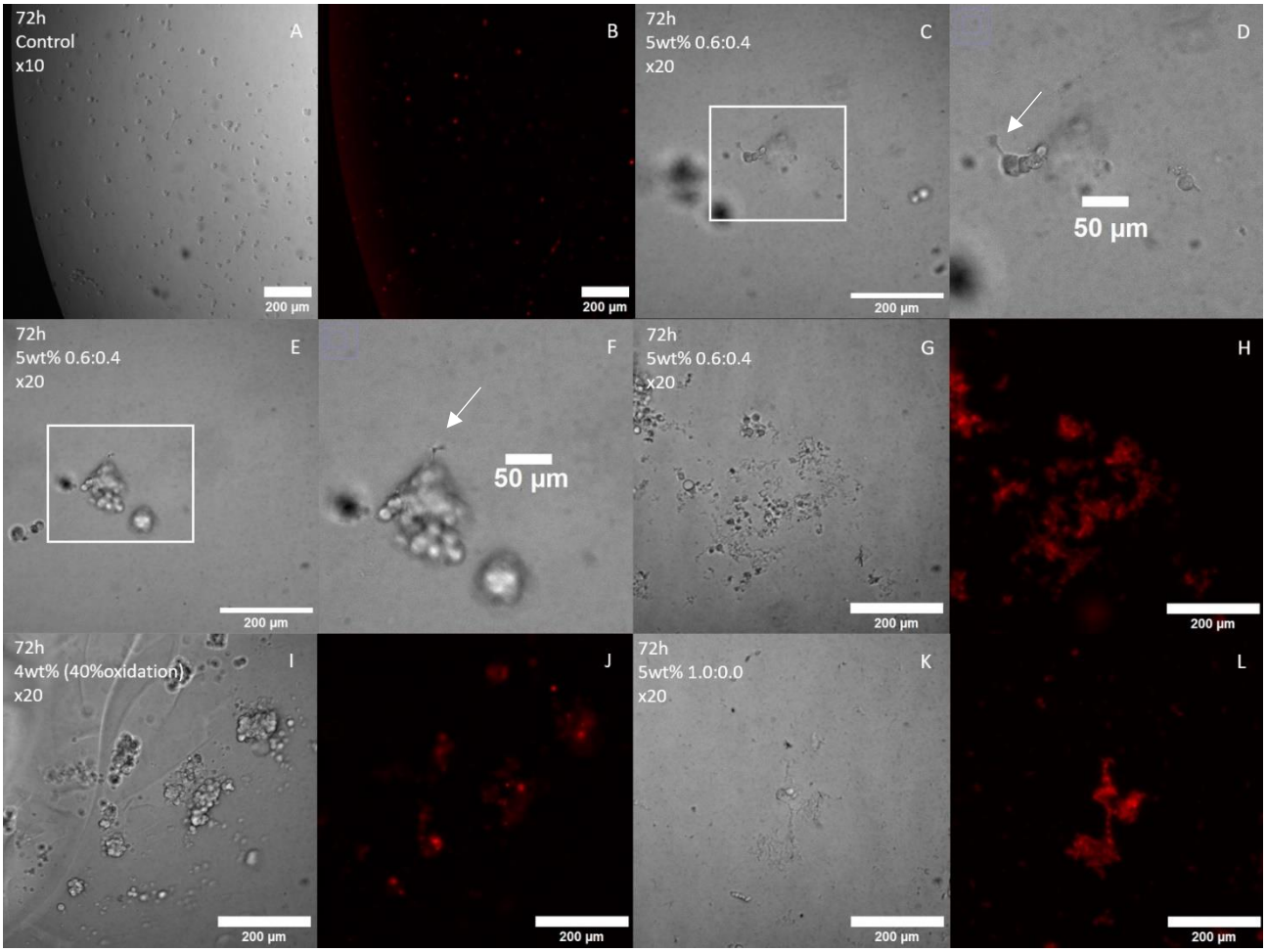

Figure 3.18 - Pictures taken in the third day of culture in the hydrogel (72h). A and B are the control groups. and in the remaining pictures it is possible to see a clear difference between the number of cells compared to the 48h pictures. C, D, E, F, G, and H correspond to pictures taken in the hydrogel with the formulation L_O.Alg_5wt%_0.6:0.4; C- Brightfield; D cell tracker image of C; E- Brightfield; F- Cell tracker image of E; G-Brightfield; H cell tracker image of H; pictures I and J were taken on the hydrogel with the formulation 40%_O.Alg_4wt%_1.0:0.0, I- Brightfield; J- Cell tracker image of J; pictures K and L were taken on the hydrogel with the formulation H_O.Alg_5wt%_1.0:0.0. In these pictures is possible to notice a decrease in the number of cells present in culture. It is also possible to notice In some of the pictures the cells clustering.

3.6.3 Live/Dead

A live/dead cell assay was performed after the first 24h of the cells seeded in the hydrogels using the cell tracker (Red) to stain all the cells and calcein AM dye (Green) to stain the live cells to ensure that the cells were not dying after being detached from where they were being differentiated and after being seeded in the hydrogels. However, other life/dead was performed after 96h of the cells being cultured in the hydrogels given that the cells did not look well after 72h. In this second live/dead assay was used Hoechst (Blue, label all live and dead cells) and Propidium Iodide (Yellow, label dead cells only). The results of both these live/dead can be seen in Figures 3.19 and 3.20. It is important to state that Morgan, *et al.* had already performed a viability test of these hydrogels in fibroblasts so the hydrogels were tought to be viable for cell survival. [30]

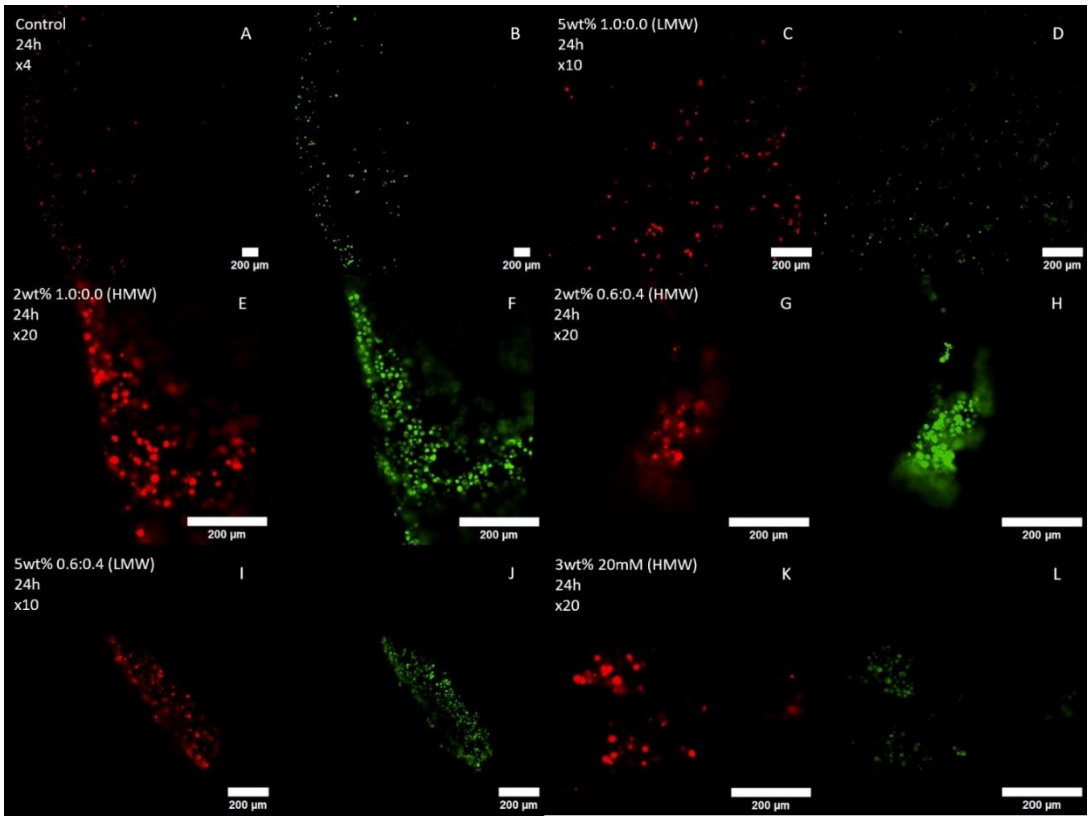

Figure 3.19 - Live/Dead performed at 24h of culture in hydrogel. In red is the fluorescent image of the cell tracker that is supposed to stain all the cells, and in green is the fluorescent image given by calcein that is staining all the live cells. A and B - Control; C and D - L_O.Alg_5wt%_1.0:0.0; E and F - H_O.Alg_2wt%_1.0:0.0; G and H - H_O.Alg_2wt%_0.6:0.4; I and J - L_O.Alg_5wt%_0.6:0.4; K and L - H_3wt%_20mMCa

The cells are indeed alive on the first 24h, but on the second life/dead assay performed it is possible to see a lot of dead cells. Another thing to notice is the clustering of cells that was not present in culture on the 48h time point, which is likely related to the cells trying to survive in a hostile environment. The number of cells was also very reduced comparing to the start of the experience, which was associated to the degradation of the hydrogels. When the hydrogels degrade the cells have no place to attach and end up being removed during the staining procedure for the live/dead assay. The cells that are still present in the well on the fourth day of culture in the hydrogel, are mostly dead, as it is possible to see from the live dead assay.

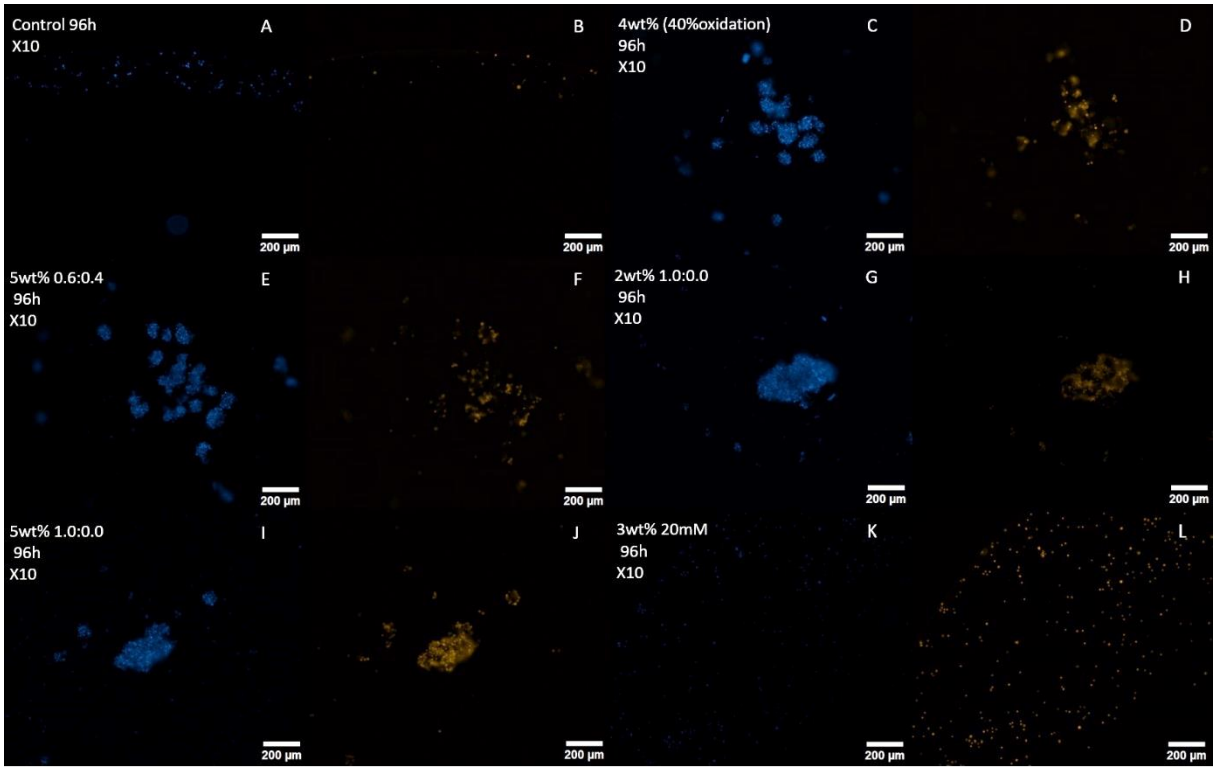

Figure 3.20 - Live/Dead performed at 96h of culture in hydrogel. The blue staining is DAPI that stains all the cells and in yellow is Propidium Iodine that stains the Dead cells. A lot of the cells were dead after 96h. A and B correspond to the control well; C and D to the 4wt% (40%oxidation) hydrogel; E and F the 5wt% LMW 0.6:0.4; G and H is the 2wt% HMW 1.0:0.0; I and J is the 5wt% LMW 1.0:0.0; and K and L correspond to the 3wt% HMW 20mM alginate crosslinked with calcium hydrogel.

The main conclusion for this is that the cells were being underfed and therefore an adjustment in the protocol needs to be made, given that a lot of dead cells were present in the control as well as in the hydrogels. The stability in culture over time was not sufficient, even though this hydrogels were capable of retaining their structure in media for a long period of time (at least two months, after that time point the hydrogels were thrown out), when cells were seeded inside the hydrogels the cell movement and metabolic activity was most likely degrading the hydrogel crosslinking at a faster past, making them only be stable in culture for 2 to 3 days.

Therefore, a new strategy must be thought to improve their culture stability over time, so that it is possible to avoid cells being washed away because of hydrogel degradation. Stability also proved crucial for cell attachment, and it is possible that it had an influence on the cells being capable of maintaining their axons. To improve this, an available approach could be to implement a double network to the hydrogels by adding a less degradable polymer and crosslinking the new polymer with a stable network. Chen et. al. prepared hydrogels composed of collagen and hyaluronic acid, crosslinked by a stable and a dynamic network, and they state to have had positive results using the PC12 cell line. [5] The interest in maintaining the oxidized alginate is because, has stated before in the project, it allows to create hydrogels with distingue mechanical properties, that could be used for culture of not only neural tissue, but for many other soft tissues. Preparing the hydrogels in a solution with collagen could help improve cell attachment, removing the necessity of adding RGD to the polymer backbone, since collagen it is an interesting material that has already been used a lot for the culture of nerve cells. After being able to optimize the stability, it would be appealing to use the nociceptor spheroids again instead of the PC12's, since the PC12's are not present in the human body, but there are nociceptors. Moreover, to improve imaging, and obtain better images in 3D the utilization of a confocal microscope would be ideal.

4

Conclusion

Throughout this project, extended material characterization was performed regarding swelling, porosity, compression, and stress-relaxation. During this project different hydrogels with different mechanical properties were obtained by varying the molecular weights and varying the crosslinkers used. The mechanical properties of these hydrogels made with oxidized alginate proved to be very versatile and demonstrated equivalent properties to various natural tissues. The range of Young Modulus values (ranging from ≈2kPa to 70 kPa) obtained for these hydrogels have similar values to the brain, kidneys, and lungs (that go from 1-10kPa). The oxidized alginate hydrogels with a 40% degree of oxidation, were able to obtain bigger values for the young modulus, reaching values close to the muscle and skin (that have values between 10-100 kPa). [27] Moreover, given the effect of oxime bonds in the increase of stiffness of these hydrogels, it is possible to say that there is a chance to achieve values that are similar to the Young modulus of the bladder and the cornea (slightly over 100kPa). There was also a slight variance in values for the alginate crosslinked with calcium (3-6kPa) varying the polymeric content and molecular weight, but they were harder to handle during the experiments without breaking or damaging the hydrogels. The stress-relaxation also proved the versatility of the oxidized alginate hydrogels, which was already expected due to past work already realized with oxidized alginate and these crosslinkers. [30] In this project an emphasis was given in altering the molecular weight of the alginate used and the polymeric content, which had not been done before. It was observed that, when decreasing the molecular weight of the polymer and increasing the polymeric content, it was possible to achieve lower values for stress-relaxation. This is interesting since several studies have stated that faster-relaxing materials help increase cell spreading and, in some cases, cell growth. [5,29] The hydrogels with higher polymeric content seemed to degrade less during culture and were easier to handle. However, stability during

culture was a consistent problem during the whole project. The hydrogels could retain their structure for several months in culture media, but they were not capable of this during culture with cells. The hydrogels with the more dynamic networks would start dissolving after three or four days of culture, and this was associated to movement and metabolic behavior of the cells. Because of that, the experiments were performed always trying to reduce the number of cells in an attempt to improve the stability of the hydrogels during culture. The degradation of the hydrogels after 3 to 4 days was noticeable to the naked eye, and it could also be seen during microscopy, this degradation would not happen so quickly without the cells. This scarcity of stability was possibly the reason for the almost non-existing axon growth seen throughout the different experiments for the nerve spheroids. Another possible explanation is the difficulty to change media during culture. The hydrogel swelling observed for a lot of the samples, and also the sandwich strategy that was being used made it difficult to change the media without touching the hydrogels with the pipette tip. This can disturb the cells, and also contribute to their detachment, and breaking of the axons. The culture strategy employed for the PC12´s allowed to reduce most of these problems, because it allowed to seed the cells in 3D without the sandwich strategy, allowing to reduce the volume of hydrogel present in each well. However, the main problem was still being the degradation of the hydrogels. It was possible to see some axon growth in a 3D environment, and by using a decent number of cells according to the space available, it was possible to avoid them clustering too much. Nonetheless, after 4 days of culture, the cells were dying. This might have been associated to the insufficient stability in culture of the hydrogels over time, but it was mostly associated to the deficit of FBS added to the culture media, given there was a lot of cell death present in the control groups as well. Therefore, it would be interesting to perfect the protocol for the culture of the PC12's, that could possibly allow the cells to survive for longer and enable them to grow more. For future work with these oxidized alginate hydrogels, it would be interesting to try and add more binding sites for the cells, for example, by blending collagen with the alginate, since collagen already presents natural binding sites for cells. Moreover, adding a double network to the hydrogels with a less degradable polymer, and a stable crosslinker could most likely allow for improvement in the hydrogels' stability over time during culture, helping in decreasing the degradation. This approach would almost certainly alter the hydrogel properties, but they would probably maintain their versatility, which makes these oxidized alginate gels with these dynamic crosslinkers a nice approach to move forward to creating different 3D scaffolds, either to culture nerves or other cells of different human tissues.

BIBLIOGRAPHY

1. Steward, M. M., Sridhar, A., & Meyer, J. S. (2013). Neural regeneration. Current topics in microbiology and immunology, 367, 163–191. https://doi.org/10.1007/82_2012_302

2. Thakur KT, Albanese E, Giannakopoulos P, et al. Neurological Disorders. In: Patel V, Chisholm D, Dua T, et al., editors. Mental, Neurological, and Substance Use Disorders: Disease Control Priorities, Third Edition (Volume 4). Washington (DC): The International Bank for Reconstruction and Development / The World Bank; 2016 Mar 14. Chapter 5. Available from: https://www.ncbi.nlm.nih.gov/books/NBK361950/ doi: 10.1596/978-1-4648-0426-7_ch5

3. Lamptey, R. N., Chaulagain, B., Trivedi, R., Gothwal, A., Layek, B., & Singh, J. (2022). A review of the common neurodegenerative disorders: current therapeutic approaches and the potential role of nanotherapeutics. International journal of molecular sciences, 23(3), 1851. https://doi.org/10.3390/ijms23031851

4. Liu, C., Fan, L., Tian, Z., Wen, H., Zhou, L., Guan, P., ... & Liu, B. (2021). Self-curling electroconductive nerve dressing for enhancing peripheral nerve regeneration in diabetic rats. Bioactive materials, 6(11), 3892-3903. https://doi.org/10.1016/j.bioactmat.2021.03.034

5. Chen, S., Liu, A., Wu, C., Chen, Y., Liu, C., Zhang, Y., ... & Fan, H. (2021). Static–Dynamic Profited Viscoelastic Hydrogels for Motor-Clutch-Regulated Neurogenesis. ACS Applied Materials & Interfaces, 13(21), 24463-24476. https://doi.org/10.1021/acsami.1c03821

6. Slaughter, B. V., Khurshid, S. S., Fisher, O. Z., Khademhosseini, A., & Peppas, N. A. (2009). Hydrogels in regenerative medicine. Advanced materials (Deerfield Beach, Fla.), 21(32-33), 3307–3329. https://doi.org/10.1002/adma.200802106

7. Du, Y., Lo, E., Ali, S., & Khademhosseini, A. (2008). Directed assembly of cell-laden microgels for fabrication of 3D tissue constructs. Proceedings of the National Academy of Sciences of the United States of America, 105(28), 9522–9527. https://doi.org/10.1073/pnas.0801866105

8. Curley, C. J., Dolan, E. B., Otten, M., Hinderer, S., Duffy, G. P., & Murphy, B. P. (2019). An injectable alginate/extra cellular matrix (ECM) hydrogel towards acellular treatment of heart failure. Drug delivery and translational research, 9(1), 1–13. https://doi.org/10.1007/s13346-018-00601-2

9. Curley, C. J., Dolan, E. B., Otten, M., Hinderer, S., Duffy, G. P., & Murphy, B. P. (2019). An injectable alginate/extra cellular matrix (ECM) hydrogel towards acellular treatment of heart failure. Drug delivery and translational research, 9(1), 1–13. https://doi.org/10.1007/s13346-018-00601-2

10. Mohammadinejad, R., Maleki, H., Larraneta, E., Fajardo, A. R., Nik, A. B., Shavandi, A., ... & Thakur, V. K. (2019). Status and future scope of plant-based green hydrogels in biomedical engineering. Applied Materials Today, 16, 213-246. https://doi.org/10.1016/j.apmt.2019.04.010

11. Saldin, L. T., Cramer, M. C., Velankar, S. S., White, L. J., & Badylak, S. F. (2017). Extracellular matrix hydrogels from decellularized tissues: Structure and function. Acta biomaterialia, 49, 1-15. https://doi.org/10.1016/j.actbio.2016.11.068

12. Society for Neuroscience. (n.d.). About neuroscience. Retrieved September 17, 2018, from https://www.brainfacts.org/core-concepts

13. Varadarajan, S. G., Hunyara, J. L., Hamilton, N. R., Kolodkin, A. L., & Huberman, A. D. (2022). Central nervous system regeneration. Cell, 185(1), 77–94. https://doi.org/10.1016/j.cell.2021.10.029

14. Wieringa, P. A., Gonçalves de Pinho, A. R., Micera, S., van Wezel, R. J., & Moroni, L. (2018). Biomimetic architectures for peripheral nerve repair: a review of biofabrication strategies. Advanced healthcare materials, 7(8), 1701164. https://doi.org/10.1002/adhm.201701164

15. Huebner, E. A., & Strittmatter, S. M. (2009). Axon regeneration in the peripheral and central nervous systems. Results and problems in cell differentiation, 48, 339–351. https://doi.org/10.1007/400_2009_19

16. Types of neurons. Queensland Brain Institute - University of Queensland. (2022, July 25). https://qbi.uq.edu.au/brain/brain-anatomy/types-neurons

17. National Institute of Neurological Disorders and Stroke. (2018). Brain basics: Know your brain. Retrieved August 9, 2018, from https://www.ninds.nih.gov/Disorders/Patient-Caregiver-Education/Know-Your-Brain

18. Dotti, C. G., Sullivan, C. A., & Banker, G. A. (1988). The establishment of polarity by hippocampal neurons in culture. The Journal of neuroscience: the official journal of the Society for Neuroscience, 8(4), 1454–1468. https://doi.org/10.1523/JNEUROSCI.08-04-01454.1988

19. Bradke, F., & Dotti, C. G. (2000). Differentiated neurons retain the capacity to generate axons from dendrites. Current biology: CB, 10(22), 1467–1470. https://doi.org/10.1016/s0960-9822(00)00807-1

20. Bradke F. (2022). Mechanisms of Axon Growth and Regeneration: Moving between Development and Disease. The Journal of neuroscience: the official journal of the Society for Neuroscience, 42(45), 8393–8405. https://doi.org/10.1523/JNEUROSCI.1131-22.2022

21. Santos, T. E., Schaffran, B., Broguière, N., Meyn, L., Zenobi-Wong, M., & Bradke, F. (2020). Axon Growth of CNS Neurons in Three Dimensions Is Amoeboid and Independent of Adhesion. Cell reports, 32(3), 107907. https://doi.org/10.1016/j.celrep.2020.107907

22. Lam, D., Enright, H. A., Cadena, J., Peters, S. K., Sales, A. P., Osburn, J. J., ... & Fischer, N. O. (2019). Tissue-specific extracellular matrix accelerates the formation of neural networks and communities in a neuron-glia co-culture on a multi-electrode array. Scientific reports, 9(1), 4159. https://doi.org/10.1038/s41598-019-40128-1

23. Li, X., Zhang, X., Hao, M., Wang, D., Jiang, Z., Sun, L., ... & Zhuo, Y. (2022). The application of collagen in the repair of peripheral nerve defect. Frontiers in Bioengineering and Biotechnology, 10, 973301. https://doi.org/10.3389/fbioe.2022.973301

24. Song, I., & Dityatev, A. (2018). Crosstalk between glia, extracellular matrix and neurons. Brain research bulletin, 136, 101–108. https://doi.org/10.1016/j.brainresbull.2017.03.003

25. Burnside, E. R., & Bradbury, E. J. (2014). Manipulating the extracellular matrix and its role in brain and spinal cord plasticity and repair. Neuropathology and applied neurobiology, 40(1), 26–59. https://doi.org/10.1111/nan.12114

26. Weltman, A., Yoo, J., & Meng, E. (2016). Flexible, penetrating brain probes enabled by advances in polymer microfabrication. Micromachines, 7(10), 180. https://doi.org/10.3390/mi7100180

27. Guimarães, C. F., Gasperini, L., Marques, A. P., & Reis, R. L. (2020). The stiffness of living tissues and its implications for tissue engineering. Nature Reviews Materials, 5(5), 351-370. https://doi.org/10.1038/s41578-019-0169-1

28. Tyler W. J. (2012). The mechanobiology of brain function. Nature reviews. Neuroscience, 13(12), 867–878. https://doi.org/10.1038/nrn3383

29. Bilston, L.E. (2011). Brain Tissue Mechanical Properties. In: Miller, K. (eds) Biomechanics of the Brain. Biological and Medical Physics, Biomedical Engineering. Springer, New York, NY. https://doi.org/10.1007/978-1-4419-9997-9_4

30. Morgan, F. L., Fernández-Pérez, J., Moroni, L., & Baker, M. B. (2022). Tuning Hydrogels by Mixing Dynamic Cross-Linkers: Enabling Cell-Instructive Hydrogels and Advanced Bio-inks. Advanced Healthcare Materials, 11(1), 2101576. https://doi.org/10.1002/adhm.202101576

31. Belkas, J. S., Shoichet, M. S., & Midha, R. (2004). Axonal guidance channels in peripheral nerve regeneration. Operative techniques in orthopaedics, 14(3), 190-198. https://doi.org/10.1053/j.oto.2004.06.001

32. Ray, W. Z., & Mackinnon, S. E. (2010). Management of nerve gaps: autografts, allografts, nerve transfers, and end-to-side neurorrhaphy. Experimental neurology, 223(1), 77-85. https://doi.org/10.1016/j.expneurol.2009.03.031

33. Moore, A. M., Kasukurthi, R., Magill, C. K., Farhadi, H. F., Borschel, G. H., & Mackinnon, S. E. (2009). Limitations of conduits in peripheral nerve repairs. Hand, 4(2), 180-186. https://doi.org/10.1007/s11552-008-9158-3

34. De Ruiter, G. C., Malessy, M. J., Yaszemski, M. J., Windebank, A. J., & Spinner, R. J. (2009). Designing ideal conduits for peripheral nerve repair. Neurosurgical focus, 26(2), E5. https://doi.org/10.3171/FOC.2009.26.2.E5

35. Dellon, A. L., & Mackinnon, S. E. (1988). An alternative to the classical nerve graft for the management of the short nerve gap. Plastic and reconstructive surgery, 82(5), 849-856. https://doi.org/10.1097/00006534-198811000-00020

36. Haddad, T., Noel, S., Liberelle, B., El Ayoubi, R., Ajji, A., & De Crescenzo, G. (2016). Fabrication and surface modification of poly lactic acid (PLA) scaffolds with epidermal growth factor for neural tissue engineering. Biomatter, 6(1), e1231276. https://doi.org/10.1080/21592535.2016.1231276

37. Iijima, Y., Ajiki, T., Murayama, A., & Takeshita, K. (2016). Effect of Artificial Nerve Conduit Vascularization on Peripheral Nerve in a Necrotic Bed. Plastic and reconstructive surgery. Global open, 4(3), e665. https://doi.org/10.1097/GOX.0000000000000652

38. Ghasemi-Mobarakeh, L., Prabhakaran, M. P., Morshed, M., Nasr-Esfahani, M. H., & Ramakrishna, S. (2010). Bio-functionalized PCL nanofibrous scaffolds for nerve tissue engineering. Materials Science and Engineering: C, 30(8), 1129-1136. https://doi.org/10.1016/j.msec.2010.06.004

39. Naghieh, S., Sarker, M. D., Abelseth, E., & Chen, X. (2019). Indirect 3D bioprinting and characterization of alginate scaffolds for potential nerve tissue engineering applications. Journal of the Mechanical Behavior of Biomedical Materials, 93, 183-193. https://doi.org/10.1016/j.jmbbm.2019.02.014

40. Baniasadi, H., SA, A. R., & Mashayekhan, S. (2015). Fabrication and characterization of conductive chitosan/gelatin-based scaffolds for nerve tissue engineering. International journal of biological macromolecules, 74, 360-366. https://doi.org/10.1016/j.ijbiomac.2014.12.014

41. Junka, R., Valmikinathan, C. M., Kalyon, D. M., & Yu, X. (2013). Laminin functionalized biomimetic nanofibers for nerve tissue engineering. Journal of biomaterials and tissue engineering, 3(4), 494-502. https://doi.org/10.1166/jbt.2013.1110

42. Navaei-Nigjeh, M., Amoabedini, G., Noroozi, A., Azami, M., Asmani, M. N., Ebrahimi-Barough, S., ... & Ai, J. (2014). Enhancing neuronal growth from human endometrial stem cells derived neuron-like cells in three-dimensional fibrin gel for nerve tissue engineering. Journal of Biomedical Materials Research Part A, 102(8), 2533-2543. https://doi.org/10.1002/jbm.a.34921

43. Itoh, S., Takakuda, K., Samejima, H., Ohta, T., Shinomiya, K., & Ichinose, S. (1999). Synthetic collagen fibers coated with a synthetic peptide containing the YIGSR sequence of laminin to promote peripheral nerve regeneration in vivo. Journal of Materials Science: Materials in Medicine, 10, 129-134. https://doi.org/10.1023/A:1008977221827

44. He, L., Zhang, Y., Zeng, C., Ngiam, M., Liao, S., Quan, D., ... & Ramakrishna, S. (2009). Manufacture of PLGA multiple-channel conduits with precise hierarchical pore architectures and in vitro/vivo evaluation for spinal cord injury. Tissue Engineering Part C: Methods, 15(2), 243-255. https://doi.org/10.1089/ten.tec.2008.0255

45. Lee, D. J., Fontaine, A., Meng, X., & Park, D. (2016). Biomimetic nerve guidance conduit containing intraluminal microchannels with aligned nanofibers markedly facilitates in nerve regeneration. ACS Biomaterials Science & Engineering, 2(8), 1403-1410. https://doi.org/10.1021/acsbiomaterials.6b00344

46. Pawar, K., Mueller, R., Caioni, M., Prang, P., Bogdahn, U., Kunz, W., & Weidner, N. (2011). Increasing capillary diameter and the incorporation of gelatin enhance axon outgrowth in alginate-based anisotropic hydrogels. Acta biomaterialia, 7(7), 2826-2834. https://doi.org/10.1016/j.actbio.2011.04.006

47. Abdelbasset, W. K., Jasim, S. A., Sharma, S. K., Margiana, R., Bokov, D. O., Obaid, M. A., ... & Mustafa, Y. F. (2022). Alginate-based hydrogels and tubes, as biological macromolecule-based platforms for peripheral nerve tissue engineering: A review. Annals of Biomedical Engineering, 50(6), 628-653. https://doi.org/10.1007/s10439-022-02955-8

48. Kloxin, A. M., Kloxin, C. J., Bowman, C. N., & Anseth, K. S. (2010). Mechanical properties of cellularly responsive hydrogels and their experimental determination. Advanced materials (Deerfield Beach, Fla.), 22(31), 3484–3494. https://doi.org/10.1002/adma.200904179

49. Lampe, K. J., Antaris, A. L., & Heilshorn, S. C. (2013). Design of three-dimensional engineered protein hydrogels for tailored control of neurite growth. Acta biomaterialia, 9(3), 5590–5599. https://doi.org/10.1016/j.actbio.2012.10.033

50. Hariyadi, D. M., & Islam, N. (2020). Current Status of Alginate in Drug Delivery. Advances in pharmacological and pharmaceutical sciences, 2020, 8886095. https://doi.org/10.1155/2020/8886095

51. Lee, K. Y., & Mooney, D. J. (2012). Alginate: properties and biomedical applications. Progress in polymer science, 37(1), 106–126. https://doi.org/10.1016/j.progpolymsci.2011.06.003

52. Aderibigbe, B. A., & Buyana, B. (2018). Alginate in Wound Dressings. Pharmaceutics, 10(2), 42. https://doi.org/10.3390/pharmaceutics10020042

53. Al-Shamkhani, A., & Duncan, R. (1995). Radioiodination of alginate via covalently-bound tyrosinamide allows monitoring of its fate in vivo. Journal of bioactive and compatible polymers, 10(1), 4-13. https://doi.org/10.1177/088391159501000102

54. Fox, M. E., Szoka, F. C., & Fréchet, J. M. (2009). Soluble polymer carriers for the treatment of cancer: the importance of molecular architecture. Accounts of chemical research, 42(8), 1141-1151. https://doi.org/10.1021/ar900035f

55. Scurtu, F., Popa, A., & Silaghi-Dumitrescu, R. (2017). Periodate-oxidized alginate as polycondensation reagent for hemoglobin. Studia Universitatis Babes-Bolyai, Chemia, 62. https://doi.org/10.24193/subbchem.2017.4.05

56. Shalapy, A., Zhao, S., Zhang, C., Li, Y., Geng, H., Ullah, S., ... & Liu, Y. (2020). Adsorption of deoxynivalenol (DON) from corn steep liquor (CSL) by the microsphere adsorbent SA/CMC loaded with calcium. Toxins, 12(4), 208. https://doi.org/10.3390/toxins12040208

57. Hafeez, S., Ooi, H. W., Morgan, F. L., Mota, C., Dettin, M., Van Blitterswijk, C., ... & Baker, M. B. (2018). Viscoelastic oxidized alginates with reversible imine type crosslinks: self-healing, injectable, and bioprintable hydrogels. Gels, 4(4), 85. ISO 690 https://doi.org/10.3390/gels4040085

58. Nikolenko, V. N., Shelomentseva, E. M., Tsvetkova, M. M., Abdeeva, E. I., Giller, D. B., Babayeva, J. V., Achkasov, E. E., Gavryushova, L. V., & Sinelnikov, M. Y. (2022). Nociceptors: Their Role in Body's Defenses, Tissue Specific Variations and Anatomical Update. Journal of pain research, 15, 867–877. https://doi.org/10.2147/JPR.S348324

59. Xie, D., Deng, T., Zhai, Z., Sun, T., & Xu, Y. (2023). The cellular model for Alzheimer's disease research: PC12 cells. Frontiers in molecular neuroscience, 15, 1016559. https://doi.org/10.3389/fnmol.2022.1016559

60. Grau, C. M., & Greene, L. A. (2012). Use of PC12 cells and rat superior cervical ganglion sympathetic neurons as models for neuroprotective assays relevant to Parkinson's disease. Methods in molecular biology (Clifton, N.J.), 846, 201–211. https://doi.org/10.1007/978-1-61779-536-7_18

61. Wiatrak, B., Kubis-Kubiak, A., Piwowar, A., & Barg, E. (2020). PC12 Cell Line: Cell Types, Coating of Culture Vessels, Differentiation and Other Culture Conditions. Cells, 9(4), 958. https://doi.org/10.3390/cells9040958

62. Wang, W.-L., Dai, R., Yan, H.-W., Han, C.-N., Liu, L.-S., & Duan, X.-H. (2015). Current Situation of PC12 Cell Use in Neuronal Injury Study. International Journal of Biotechnology for Wellness Industries, 4(2), 61–66. https://doi.org/10.6000/1927-3037.2015.04.02.3

63. Hu, R., Cao, Q., Sun, Z., Chen, J., Zheng, Q., & Xiao, F. (2018). A novel method of neural differentiation of PC12 cells by using Opti-MEM as a basic induction medium. *International journal of molecular medicine*, *41*(1), 195–201. https://doi.org/10.3892/ijmm.2017.3195

64. Jeon, C. Y., Jin, J. K., Koh, Y. H., Chun, W., Choi, I. G., Kown, H. J., Kim, Y. S., & Park, J. B. (2010). Neurites from PC12 cells are connected to each other by synapse-like structures. Synapse (New York, N.Y.), 64(10), 765–772. https://doi.org/10.1002/syn.20789

65. Matyash, M., Despang, F., Ikonomidou, C., & Gelinsky, M. (2014). Swelling and mechanical properties of alginate hydrogels with respect to promotion of neural growth. Tissue Engineering Part C: Methods, 20(5), 401-411. https://doi.org/10.1089/ten.tec.2013.0252

66. Savić Gajić, I. M., Savić, I. M., & Svirčev, Z. (2023). Preparation and Characterization of Alginate Hydrogels with High Water-Retaining Capacity. Polymers, 15(12), 2592. https://doi.org/10.3390/polym15122592

67. Chaudhuri, O., Gu, L., Klumpers, D., Darnell, M., Bencherif, S. A., Weaver, J. C., Huebsch, N., Lee, H. P., Lippens, E., Duda, G. N., & Mooney, D. J. (2016). Hydrogels with tunable stress relaxation regulate stem cell fate and activity. Nature materials, 15(3), 326–334. https://doi.org/10.1038/nmat4489

68. Malheiro, A., Morgan, F., Baker, M., Moroni, L., & Wieringa, P. (2020). A three-dimensional biomimetic peripheral nerve model for drug testing and disease modelling. Biomaterials, 257, 120230. https://doi.org/10.1016/j.biomaterials.2020.120230

69. Mazzeo, M. S., Chai, T., Daviran, M., & Schultz, K. M. (2019). Characterization of the Kinetics and Mechanism of Degradation of Human Mesenchymal Stem Cell-Laden Poly(ethylene glycol) Hydrogels. ACS applied biomaterials, 2(1), 81–92. https://doi.org/10.1021/acsabm.8b00390

A

STATISTICAL ANALYSIS

A.1 Young Modulus before and after swelling

2wt%0.6:0.4 Swell	2wt%0.6:0.4
6.798421839	4.78446
9.021350318	4.706476
8.075487913	2.283698
	6.853321
	4.617387

t-Test: Two-Sample Assuming Unequal Variances

	2wt%0.6:0.4 Swell	*2wt%0.6:0.4*
Mean	7.96508669	4.64906848
Variance	1.244494078	2.619084322
Observati	3	5
Hypothes	0	
df	6	
t Stat	3.422673525	
P(T<=t) or	0.007048687	
t Critical	1.943180281	
P(T<=t) tw	0.014097374	
t Critical t	2.446911851	

2wt%0100	2wt%0100 Swell
1.210843554	3.705659038
2.632687702	1.322542406
2.293739872	
4.157771682	
3.387418196	

t-Test: Two-Sample Assuming Unequal Variances

	2wt%0100	*2wt%0100 Swell*
Mean	2.736492201	2.514100722
Variance	1.244537202	2.839622442
Observati	5	2
Hypothes	0	
df	1	
t Stat	0.172157752	
P(T<=t) or	0.445732445	
t Critical	6.313751515	
P(T<=t) tw	0.891464891	
t Critical t	12.70620474	

5wt%0604	5wt%0604 Swell
15.09422281	40.03164
30.13722913	32.64054
15.13951399	25.44722
18.41423761	24.79043
26.90052599	34.50012

t-Test: Two-Sample Assuming Unequal Variances

	5wt%0604	*5wt%0604 Swell*
Mean	21.1371459	31.48198807
Variance	48.53019642	41.18583692
Observati	5	5
Hypothes	0	
df	8	
t Stat	-2.442158457	
P(T<=t) or	0.020214083	
t Critical	1.859548038	
P(T<=t) tw	0.040428167	
t Critical t	2.306004135	

5wt%1.0:0.0	5wt%1.0:0.0Swell
6.070304772	6.247100833
11.09585828	4.845187231
7.511859543	2.208390424
14.59968066	4.077793625
6.747820881	

t-Test: Two-Sample Assuming Unequal Variances

	5wt%1.0:0.0	*5wt%1.0:0.0Swell*
Mean	9.205104827	4.344618028
Variance	12.8521731	2.83489133
Observati	5	4
Hypothes	0	
df	6	
t Stat	2.684099633	
P(T<=t) or	0.018168556	
t Critical	1.943180281	
P(T<=t) tw	0.036337111	
t Critical t	2.446911851	

3wt%20mM	3wt%20mMSwell
0.746617848	17.38515
4.901062684	7.701913
1.556076475	6.863151
6.410920588	
5.138234784	

t-Test: Two-Sample Assuming Unequal Variances

	3wt%20mM	*3wt%20mMSwell*
Mean	3.750582476	10.65007069
Variance	6.041560645	34.19682674
Observati	5	3
Hypothes	0	
df	2	
t Stat	-1.943151308	
P(T<=t) or	0.095732193	
t Critical	2.91998558	
P(T<=t) tw	0.191464385	
t Critical t	4.30265273	

10wt%20mM	10wt% Swell
5.100278431	0.171053401
5.31887663	3.395095142
3.85056278	3.095396324
6.36557921	
10.27243582	

t-Test: Two-Sample Assuming Unequal Variances

	10wt%20mM	*10wt% Swell*
Mean	6.181546574	2.220514956
Variance	6.029017129	3.172674344
Observati	5	3
Hypothes	0	
df	6	
t Stat	2.632881683	
P(T<=t) or	0.019454622	
t Critical	1.943180281	
P(T<=t) tw	0.038909244	
t Critical t	2.446911851	

Above are the t-student analysis done on the data regarding the young modulus of the hydro-gels before and after swelling. It is shown that the young modulus differences before and after swelling are significant for the 2wt%0.6:0.4; 5wt%0.6:0.4; 5wt%1.0:0.0; and 10wt% 20mM. When the test is done for $p \leq 0.05$.

A.2 Ultimate compression stress

5wt% 1.0:0.0	2WT%1.0:0.0
0.11	0.138
0.08	0.093
0.062	0.082

t-Test: Two-Sample Assuming Unequal Variances

	5wt% 1.0:0.0	*2WT%1.0:0.0*
Mean	0.084	0.104333
Variance	0.000588	0.00088
Observati	3	3
Hypothes	0	
df	4	
t Stat	-0.91909	
P(T<=t) or	0.205029	
t Critical (	2.131847	
P(T<=t) tw	0.410058	
t Critical t	2.776445	

2WT%1.0:0.0	*2wt%0.6:0.4*
0.138	0.095
0.093	0.085
0.082	0.066
	0.061

t-Test: Two-Sample Assuming Unequal Variances

	2WT%1.0:0.0	*2wt%0.6:0.4*
Mean	0.104333	0.07675
Variance	0.00088	0.000255
Observati	3	4
Hypothes	0	
df	3	
t Stat	1.45951	
P(T<=t) or	0.120265	
t Critical (	2.353363	
P(T<=t) tw	0.240531	
t Critical t	3.182446	

5wt%0.6:0.4	*5wt%0.6:0.4 swell*
0.089	0.0288
0.046	0.025
0.061	0.0207
0.065	0.032
0.05	

t-Test: Two-Sample Assuming Unequal Variances

	5wt%0.6:0.4	*%0.6:0.4 swell*
Mean	0.0622	0.026625
Variance	0.000285	2.38E-05
Observati	5	4
Hypothes	0	
df	5	
t Stat	4.486043	
P(T<=t) or	0.003241	
t Critical (	2.015048	
P(T<=t) tw	0.006482	
t Critical t	2.570582	

Doing the t-student test for the different ultimate compression values it was possible to conclude that were was no significant variance of the values when changing the crosslinkers or the polymer content of the hydrogels. There was however a significant change of the ultimate compression stress before and after swelling.

B

Cell Culture

B.1 Nerve Spheroids

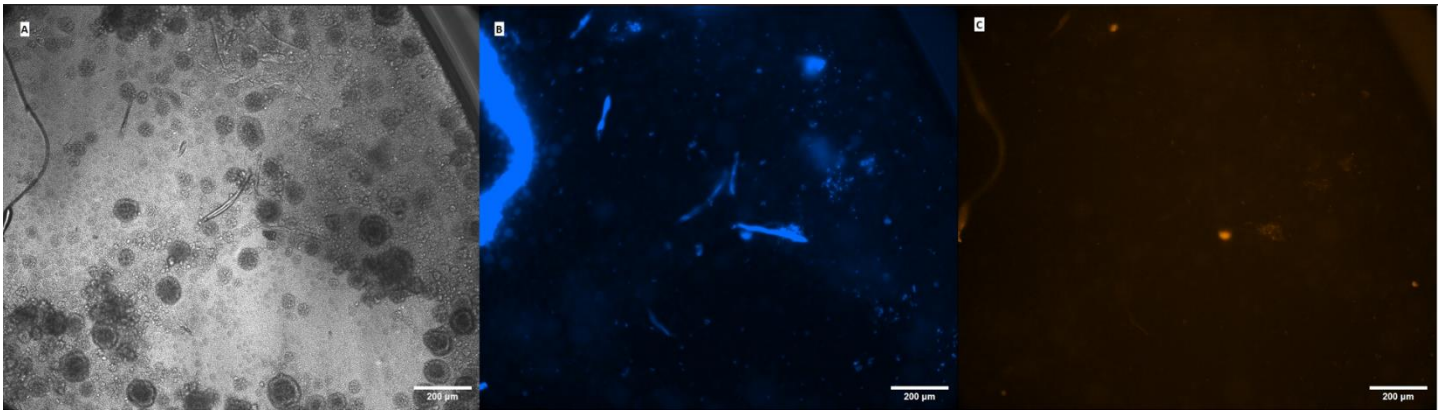

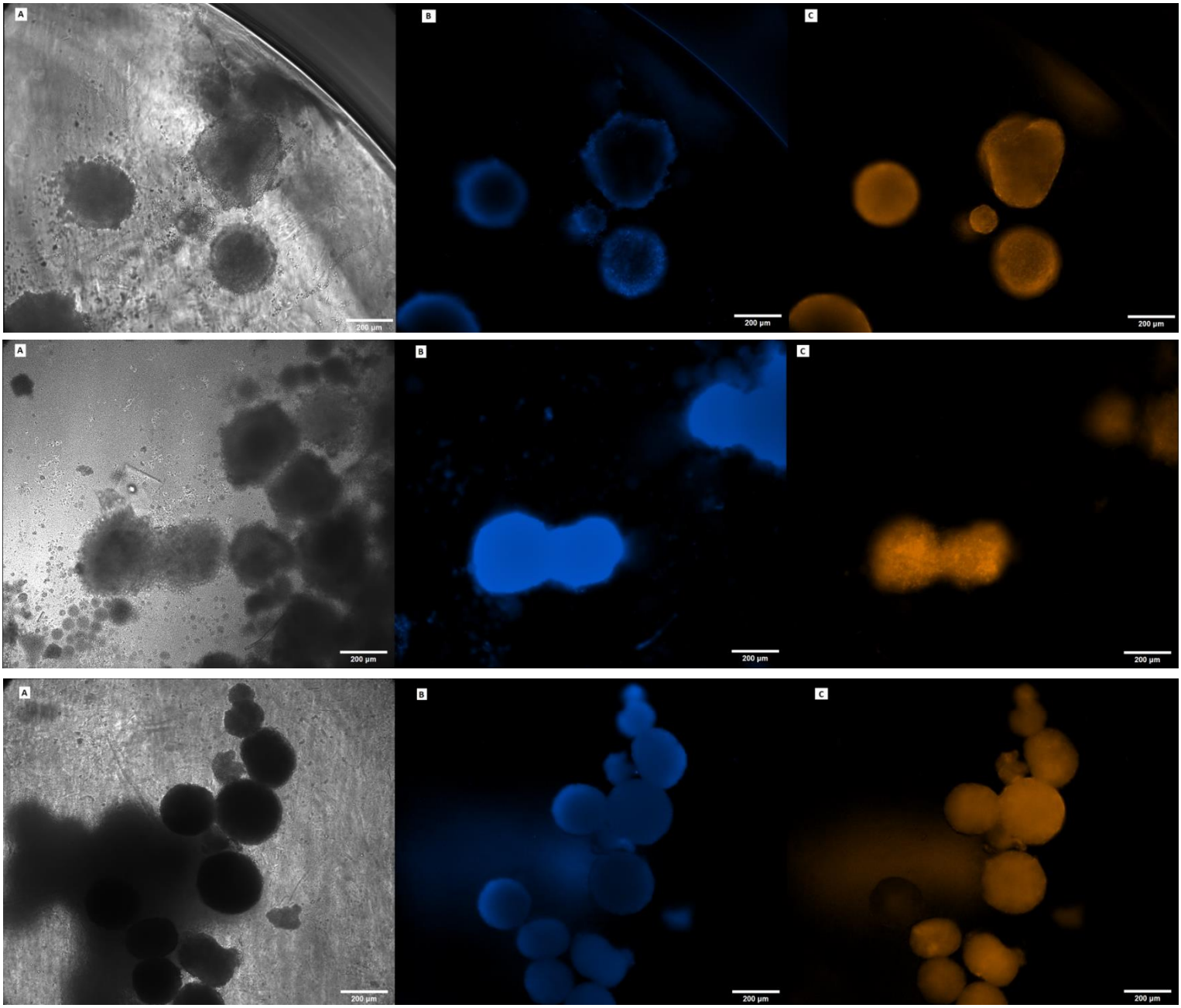

Pictures of the nerve spheroids where It can also be seen again what was mentioned in the thesis

B.2 PC12´s

Pictures of the PC12's taken at the 48h timepoint.

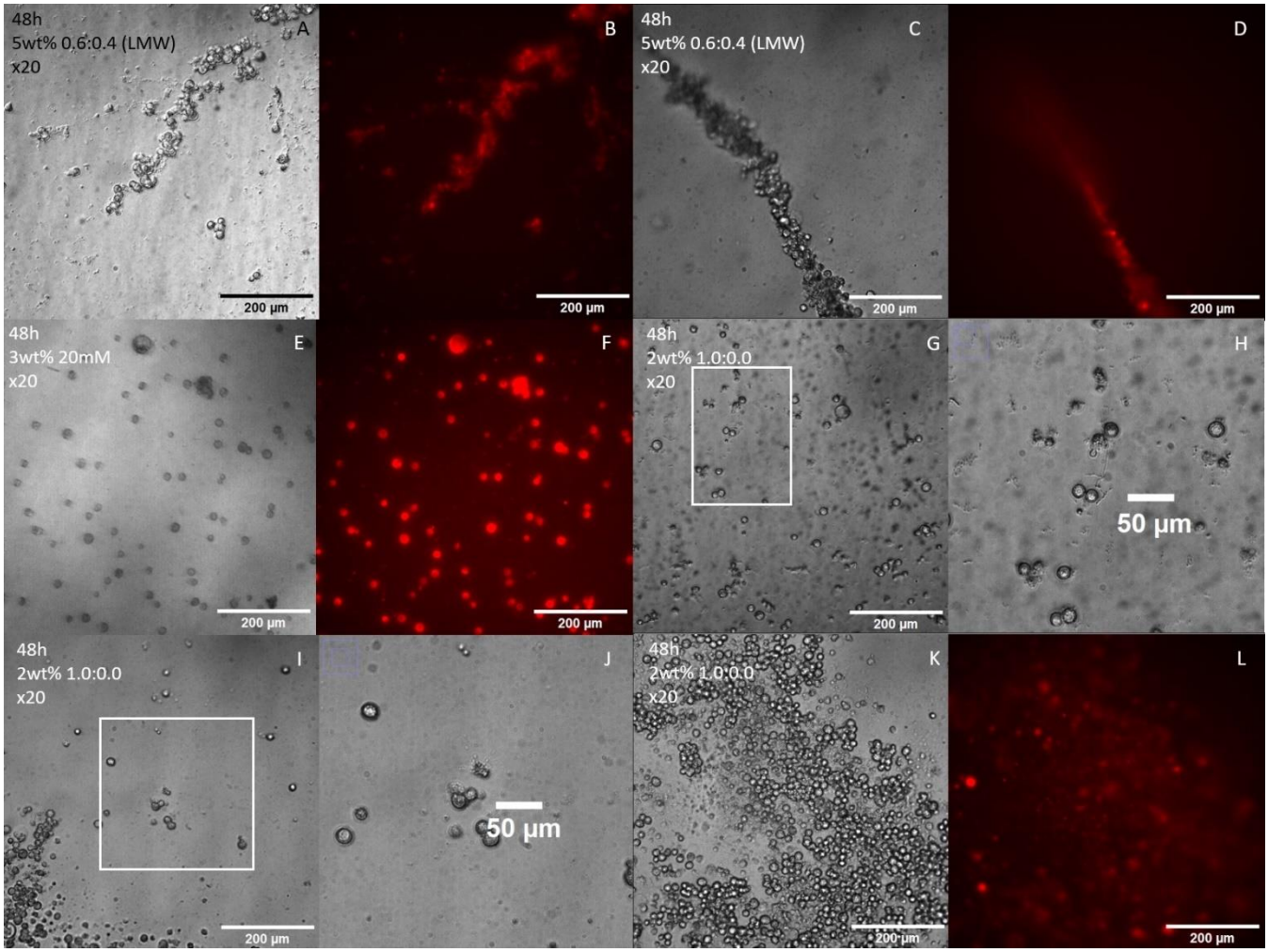

Pictures of the PC12's taken at the 72h timepoint.

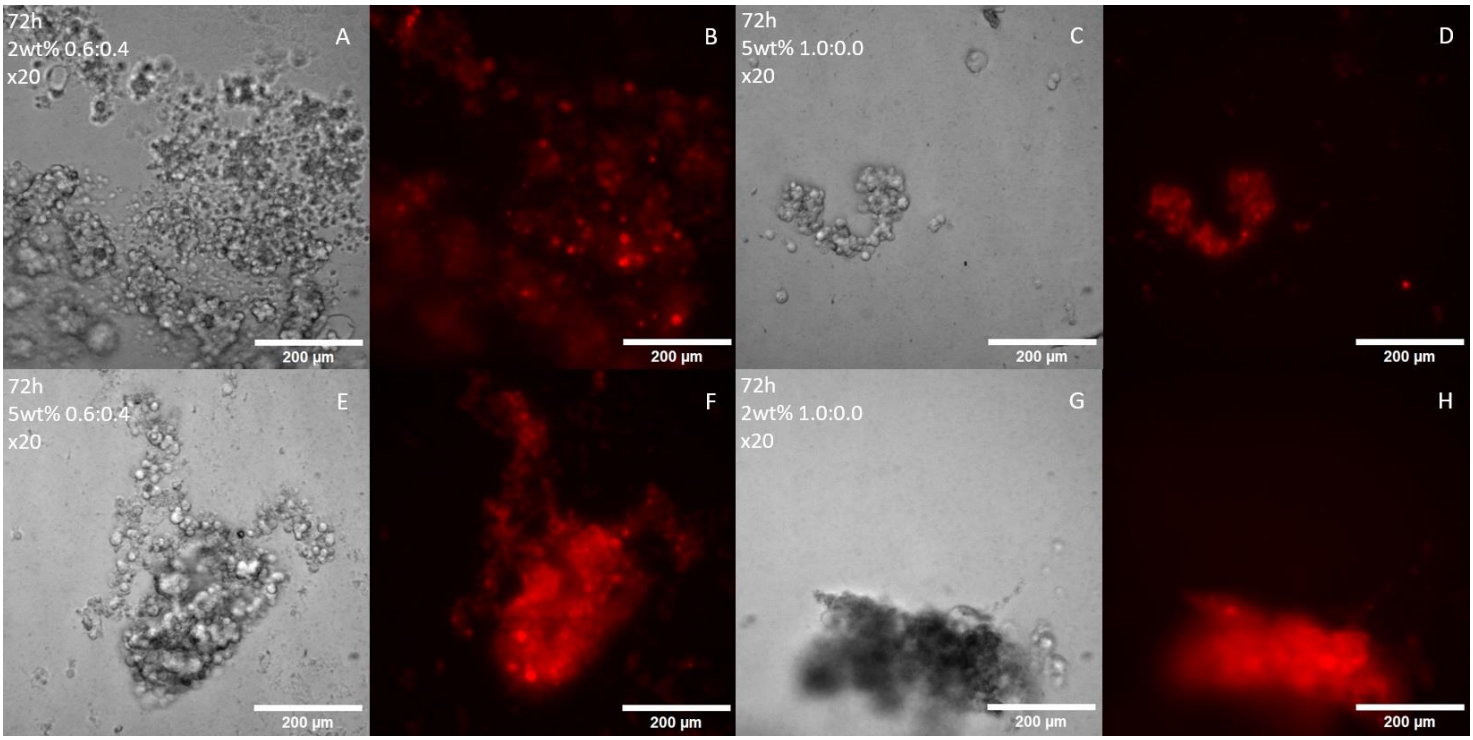

C

NUCLEIC MAGNETIC RESONANCE

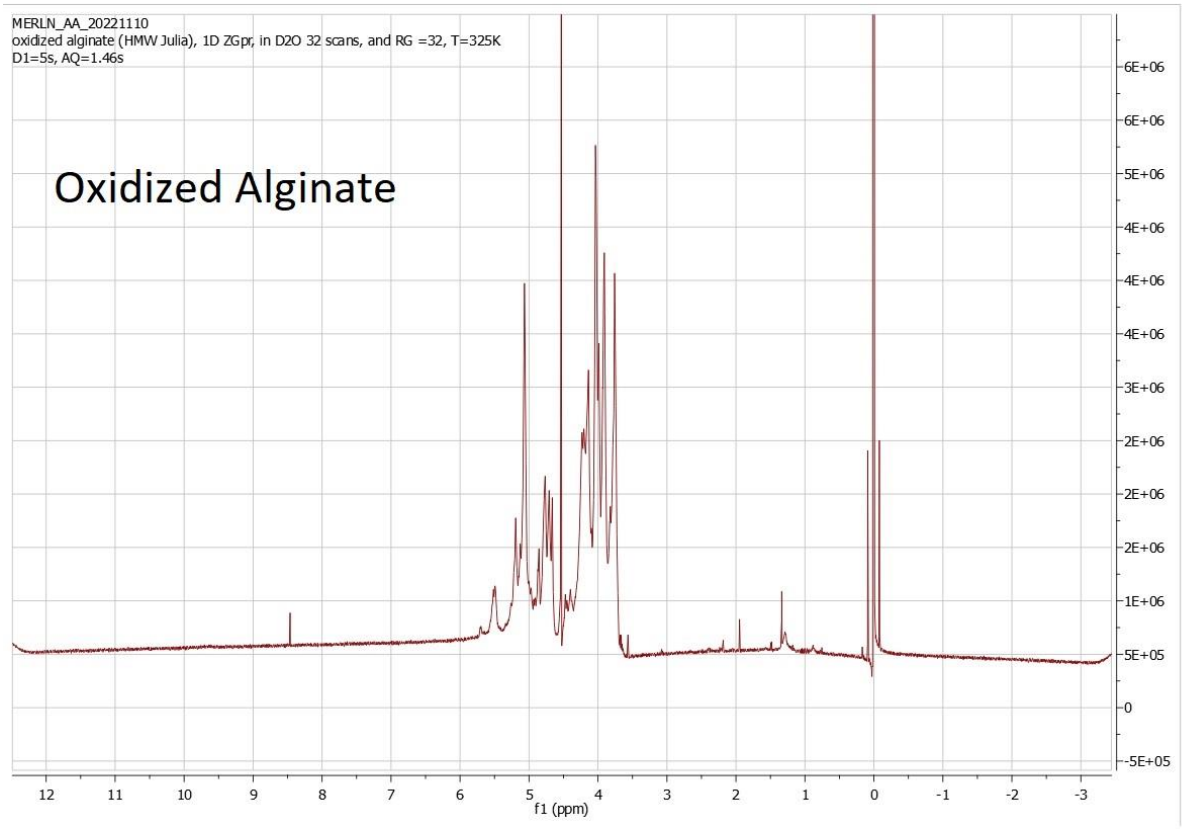

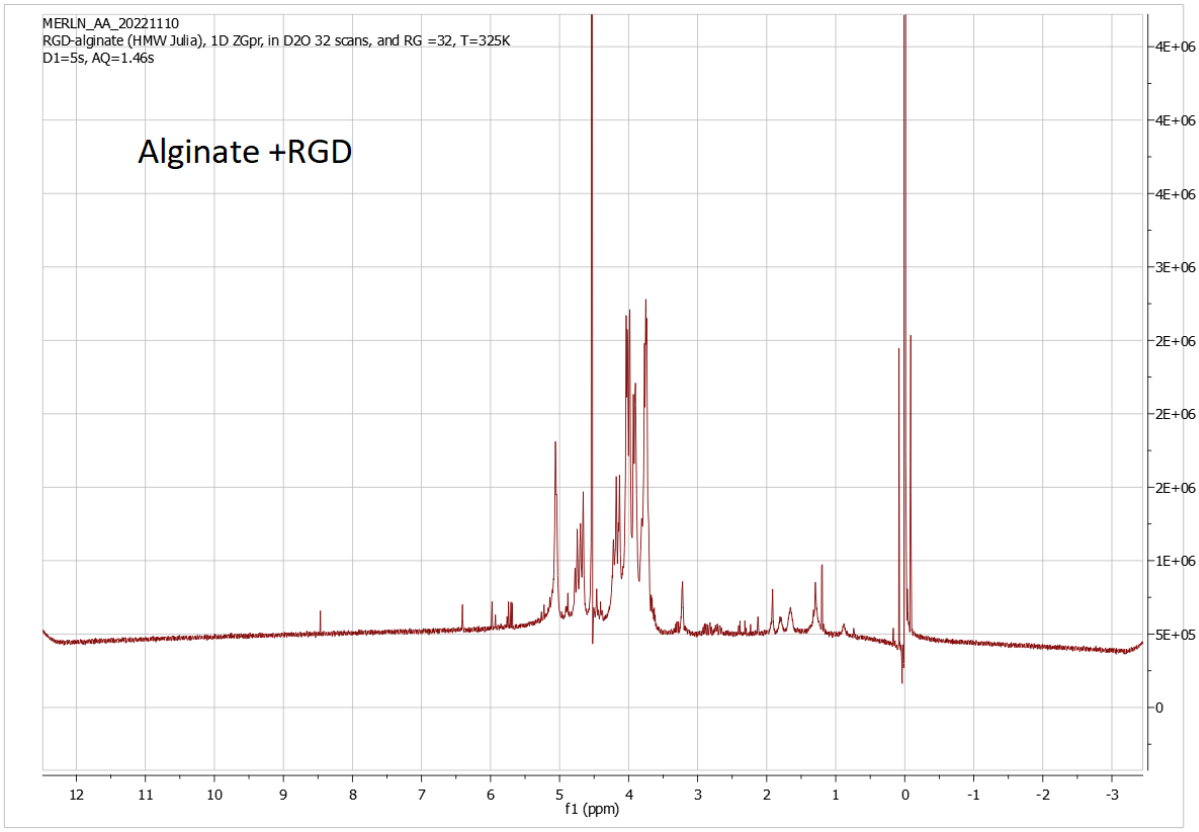
MERLN_AA_20221110
RGD-alginate (HMW Julia), 1D ZGpr, in D2O 32 scans, and RG =32, T=325K
D1=5s, AQ=1.46s
Alginate +RGD
4E+06
4E+06
4E+06
3E+06
2E+06
2E+06
2E+06
1E+06
5E+05
0
12 11 10 9 8 7 6 5 4 3 2 1 0 -1 -2 -3
f1 (ppm)

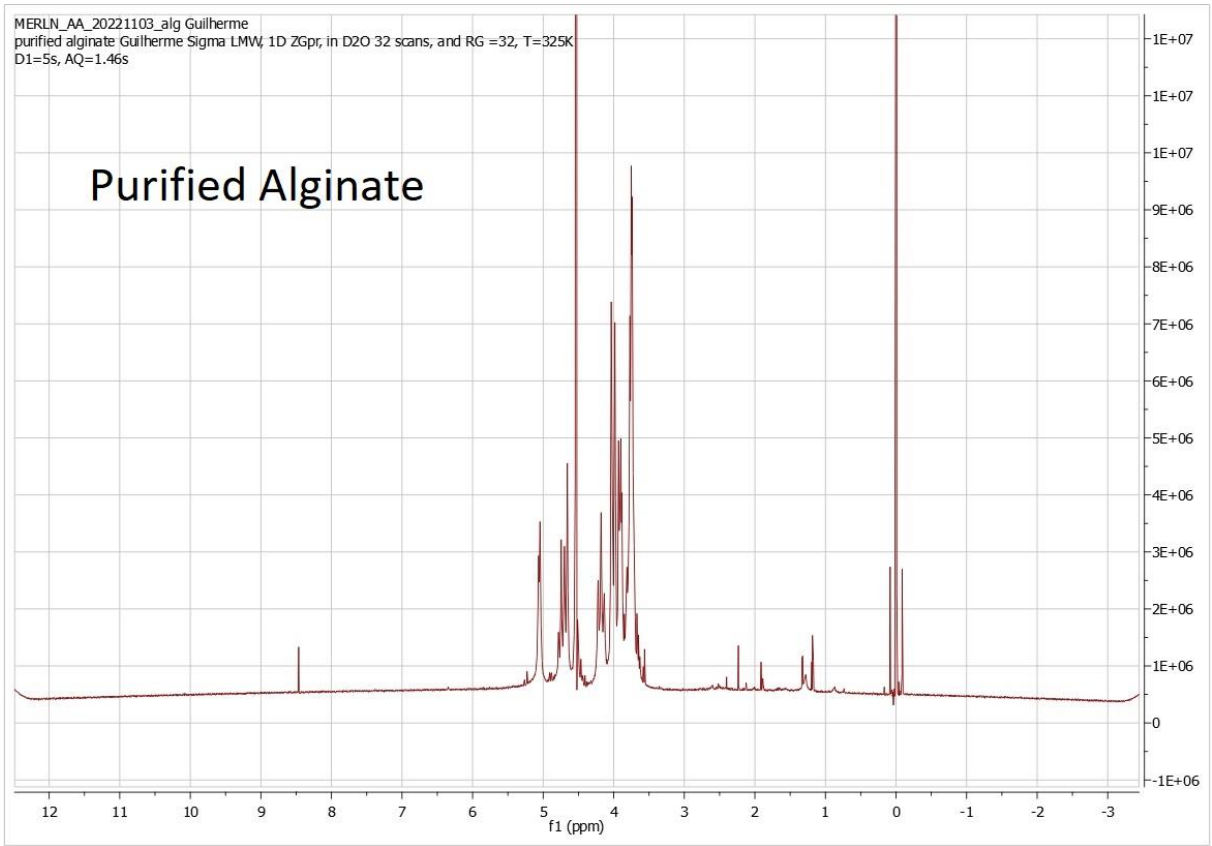
MERLN_AA_20221103_alg Guilherme
purified alginate Guilherme Sigma LMW, 1D ZGpr, in D2O 32 scans, and RG =32, T=325K
D1=5s, AQ=1.46s
Purified Alginate
1E+07
1E+07
1E+07
9E+06
8E+06
7E+06
6E+06
5E+06
4E+06
3E+06
2E+06
1E+06
0
-1E+06
12 11 10 9 8 7 6 5 4 3 2 1 0 -1 -2 -3
f1 (ppm)

D

Original Compression and Stress-Relaxation graphs and hydrogel formulations

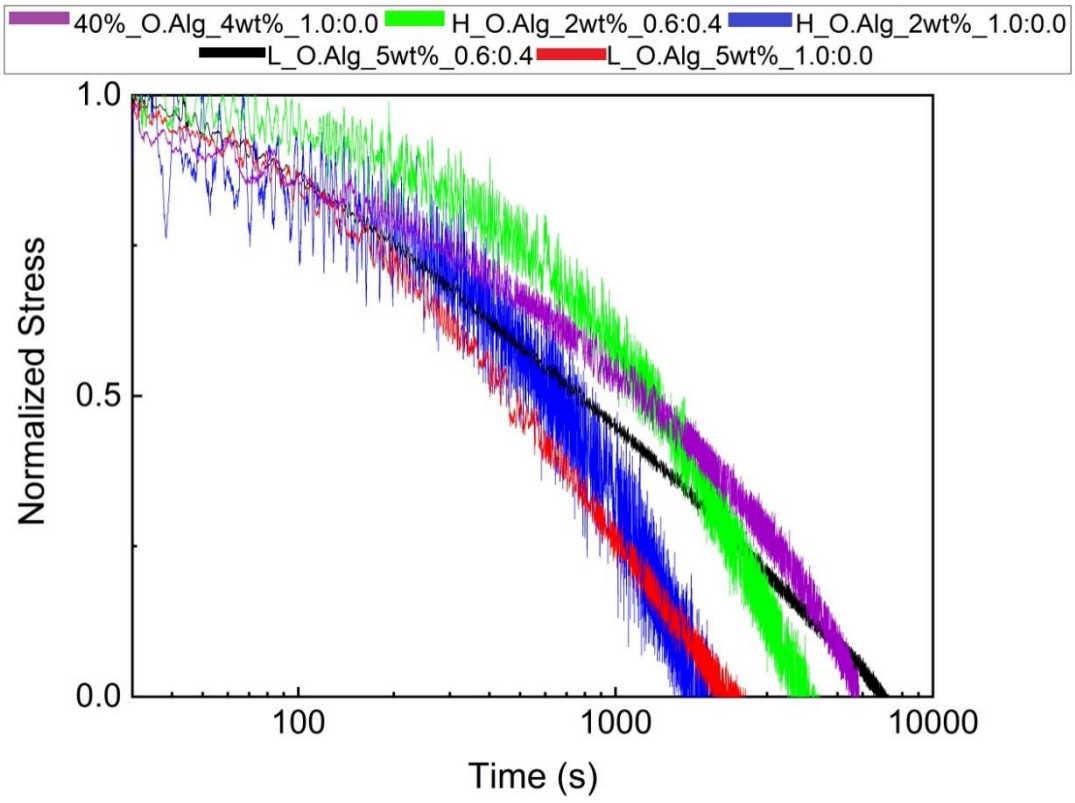

Original Stress-Relaxation graph, to make it easier to analyze in the thesis are represented the trend lines of this data.

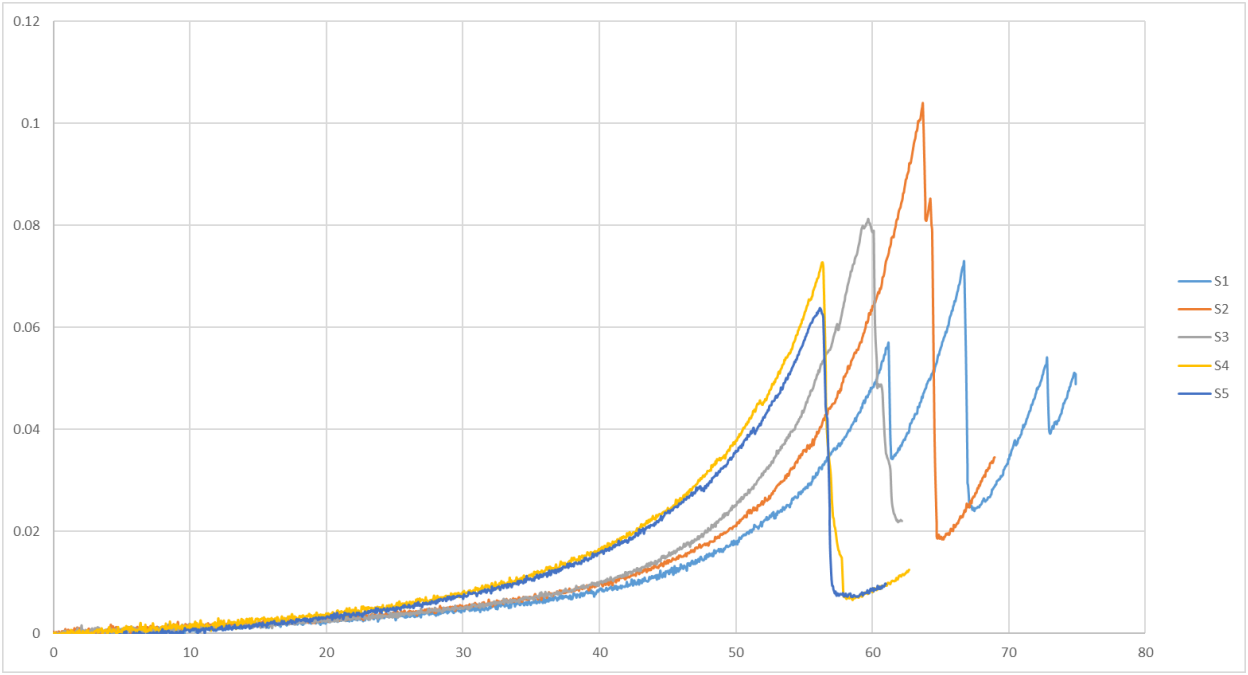

Example of the graphs obtained while doing compression, with these graphs it is possible to obtain information relative to the maximum stress before complete failure of the hydrogel and also the young modulus values that were obtained from the slop of the points in the region from 10-20%.

HMW Alginate	LMW Alginate	HMW O.Alg	LMW O.Alg
1wt% 20mM and 40mM	7.5wt% 20mM and 40mM	2wt% (1.0:0.0) and (0.6:0.4)	4wt% (1.0:0.0)
2wt% 20mM and 40mM	10wt% 20mM and 40mM	40% Oxidized 3wt% (1.0:0.0)	5wt% (1.0:0.0) (0.80.2) (0.7:0.3) (0.6:0.4)
3wt% 20 mM and 40 mM		40% Oxidized 4wt% (1.0:0.0)	6wt% (1.0:0.0)
			7wt% (1.0.0.0)